EUROPEAN COMMISSION

Community Research

SEVENTH FRAMEWORK PROGRAMME

CARBOWASTE

Treatment and Disposal of Irradiated Graphite and Other Carbonaceous Waste

Grant Agreement Number: FP7-211333

Deliverable D-4.3.4

Decontamination Factors by Steam Reforming

Author(s):

Benjamin Kraus, Dirk Vulpius, Christian Fischer, Corrado Rizzato

Forschungszentrum Jülich GmbH (Germany)

Document Number: CARBOWASTE-1301-D-4.3.4

Date of issue of this report: 31/01/2013

Project co-funded by the European Commission under the Seventh Framework Programme (2007 to 2011) of the European Atomic Energy Community (EURATOM) for nuclear research and training activities		
Dissemination Level		
PU	Public	
RE	Restricted to the partners of the CARBOWASTE project	
CO	Confidential, only for specific distribution list defined on this document	**X**

Start date of project: **01/04/2008** Duration: **60 Months**

Distribution list

Person and organisation name and/or group	Comments
WP4 members	
Executive Board	
Co-ordinator	

CARBOWASTE		
Work package: 4 **Task:** 4.3	**CARBOWASTE document no:** CARBOWASTE-1301-D-4.3.4 (e.g. May 2008 as date of issue: 0805)	**Document type:** D = Deliverable
Issued by: Forschungszentrum Jülich GmbH (DE) **Internal no.:** CW1301-Deliverable-4-3-4-b.doc		**Document status:** Draft/Review/Final

Document title

Decontamination Factors by Steam Reforming

Executive summary

Revisions

Rev.	Date	Short description	Author	Internal Review	Task Leader	WP Leader
00	dd/mm/yyyy	Issue	Name, Organisation	Name, Organisation *Signature*	Name, Organisation *Signature*	Name, Organisation *Signature*
01	dd/mm/yyyy	First issue	Kraus FZJ	von Lensa FZJ	Vulpius FZJ	Vulpius FZJ
02	dd/mm/yyyy	2nd Issue	Fischer FZJ	Von Lensa FZJ	Vulpius FZJ	Vulpius FZJ

Table of Content

1. INTRODUCTION 6

2. GRAPHITE 7

2.1 Graphite in nuclear applications 8
2.1.1 Research Reactor FRJ-1 Merlin 10
2.1.2 Research reactor FRJ-2 DIDO 11
2.1.3 High-temperature nuclear reactors 12
2.1.4 Gas –cooled reactors 13

2.2 Graphite as nuclear waste 15
2.2.1 Carbon-14 15
2.2.2 Tritium 15
2.2.3 Other radionuclides 16
2.2.4 Activity inventory 17
2.2.5 Disposal of irradiated reactor graphites 18

2.3 Decontamination procedures for irradiated nuclear graphite 20
2.3.1 Treatment processes 20
2.3.2 Steam reactions with graphite solid bodies 20
2.3.3 Determination of radionuclide release 24

3. MATERIAL & METHODS 25

3.1 Steam reforming installation 25
3.1.1 Equipment 25
3.1.2 Reagents 26
3.1.3 Installation description 27

3.2 Materials investigated and sample preparation 28
3.2.1 DIDO graphite 28
3.2.2 Irradiated Merlin graphite 28
3.2.3 Irradiated Saint Laurent Graphite 29

3.3 Treatment and analysis of graphite 30
3.3.1 Experimental parameters and treatment operations 30
3.3.1.1 Virgin DIDO graphite 30
3.3.1.2 Merlin graphite 31
3.3.1.3 Saint Laurent graphite 32
3.3.2 Liquid scintillation counting 33

4. RESULTS 34

4.1 System test 34

4.2 Experiments with virgin DIDO graphite 35

4.3 Experiments with irradiated Merlin graphite 36

4.3.1 Performance of experiments 36
4.3.2 Release of carbon-14 36
4.3.3 Release of tritium 40
4.3.4 Mass spectrometer results 43
4.3.5 Determination of decontamination factors 45

4.4 Experiments with irradiated Saint Laurent graphite **47**
4.4.1 Performance of experiments 47
4.4.2 Release of carbon-14 47
4.4.3 Release of tritium 49
4.4.4 Determination of decontamination factors 50

5. SUMMARY **52**

6. REFERENCES **55**

A. APPENDIX **57**

A.1 Activity inventories of other nuclear graphites **57**
A.1.1 Irradiated DIDO graphite 57
A.1.2 Irradiated Merlin graphite 57
A.1.3 Irradiated Saint-Laurent A2 graphite 58
A.1.4 Irradiated RBMK graphite 58

A.2 Summary of thermal treatment with decontamination factors **59**

A.3 List of figures **60**

A.4 List of tables **61**

1. Introduction

Graphite is a very important material in nuclear applications because of its physical properties and thermal and mechanical durability. Therefore it can be used as reflector, moderator, fuel matrix and construction material [FLO09] [POD04].
During the operation in nuclear reactors graphite gets irradiated and acquires radioactive materials. The acquired activity is high enough to declare nuclear graphite as nuclear waste. In Germany, the current waste-management strategy for carbonaceous radioactive is an optimized packing concept in deep geological formations [FAC08] [BfS]. The large volume of irradiated graphite and carbon bricks is reducing the cost efficiency of this strategy, because the bulk amount is inactive ^{12}C [FAC08]. Another problem is the content of longlived radioisotopes (e.g. ^{14}C, ^{36}Cl) [EUR08].
To find a solution to these waste and volume problems EURATOM proclaimed the project CARBOWASTE, which focuses on treatment and disposal of irradiated graphite and other carbonaceous waste.
Within the framework of CARBOWASTE Podruzhina's dissertation "Graphite as radioactive waste: Corrosion behavior under final repository conditions and thermal treatment" was one of the first showing that a steam reformation of graphite might work. Hence this work is based on Podruzhina's dissertation and focuses on the decontamination of irradiated nuclear graphite (i-graphite) by steam reforming.

The main objectives of this thesis were:

- performing a system test with tube furnace Carbolite STF 15/-/180 and carry out experiments with a connected humidity generator to gain knowledge about the treatment method of steam reforming with varying parameters of temperature, humidity and duration of treatment.
- determine decontamination factors concerning ^{3}H and ^{14}C of steam reformed irradiated nuclear graphite.

The further goal of these experiments on irradiated nuclear graphite is developing a prototype installation for the decontamination of graphite so the radioactive waste has a lower volume and eventually the graphite can be reused.

2. Graphite

Graphite is a natural occurring form of carbon. It builds flat layers with poly-cyclic rings of six carbon atoms. These parallel layers are bonded by weak van der Waals forces.

The layer distance is 335 pm, while carbon atoms between each other have a distance of 141.5 pm. Every carbon atom has a bond to three other carbon atoms via -bonding. Therefore one free electron is available to every carbon atom to build a delocalized π-bonding-system. These free electrons are responsible for graphite's good conductivity.

There are two different modifications of graphite due to different stratification:

- α-graphite (hexagonal crystallization)
- β-graphite (rhombohedral crystallization)

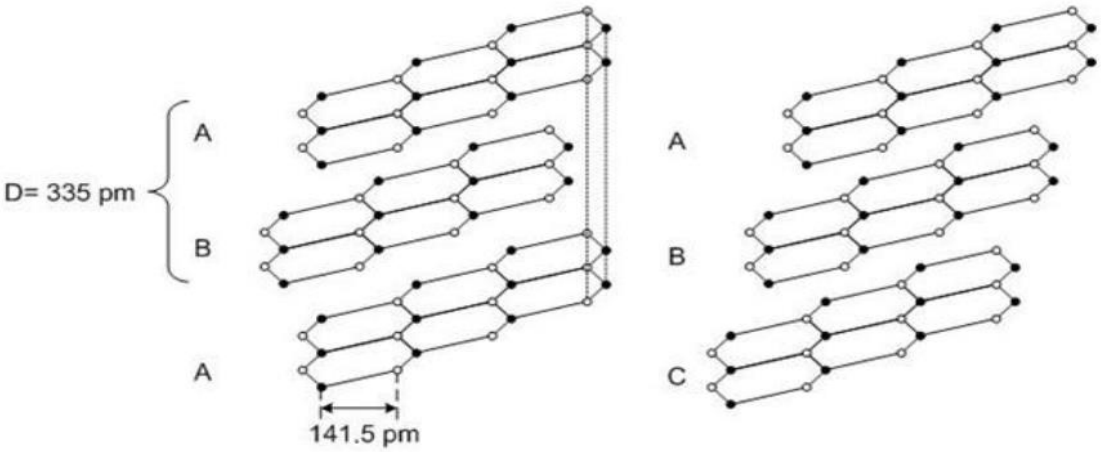


Figure 2.1: α-Graphite (left) and β-graphite (right) [FIS12]

2.1 Graphite in nuclear applications

Graphite was widely used within nuclear reactors till the 1990s. It is an important construction material in nuclear reactor design, because it retains its properties at high temperatures concerning [FLO09] [FIS12]:

- high resistance to thermal shocks
- good thermal conductivity
- low coefficient of thermal expansion
- low cross section of neutron absorption
- good mechanic machinability

Nuclear graphite in nuclear reactors needs to be free of boron or other neutron absorbing materials, because these would hinder a proper nuclear fission. Hence the content of neutron absorbing materials should be less than 5 ppm.
In Germany, nuclear graphite was used in the pebble bed reactors as construction material, reflector material and nuclear fuel coating. Another use of nuclear graphite is the Russian RBMK where it was used as a moderator.
In its natural form, graphite cannot be used for nuclear applications. It needs to be specifically manufactured according to its intended use.
The production of graphite consists building the “green body” (see below), pyrolyzing beneath 1300 °C, increasing of the density by impregnation and finally, graphitization at 2500 °C to enforce the binder’s crystallization.
The green body is a shapeable compound of coke grains and carbonaceous binders like pitch and tar. There are different methods of shaping and pressing to influence the conductivity of graphite, especially when it comes to the design of moderator and reflector materials.
A secondary pyrolysis at 1000 °C begins to extract the binders after the green body was molded; because of the pyrolysis carbon bridging occurs which leads to a homogeneous graphite mold. Subsequently, the graphite mold is covered with a carbonaceous impregnator to close the porosities. The final graphitization at 2500 °C to 3000 °C should cater for the crystallization. In this step, density is increased and impurities are removed. If coke grains are

not perfectly crystallized, there will be great discrepancies between the graphite layers which lead to a lower oxidation resistance within the mold.

Despite the previous mentioned production processes, the graphite mold still has a great number of porosities which are categorized by the following diameters according to [DEL83]:

- micropore: d < 2 nm
- mesopore: 2 nm < d < 50 nm
- macropore: 50 nm < d

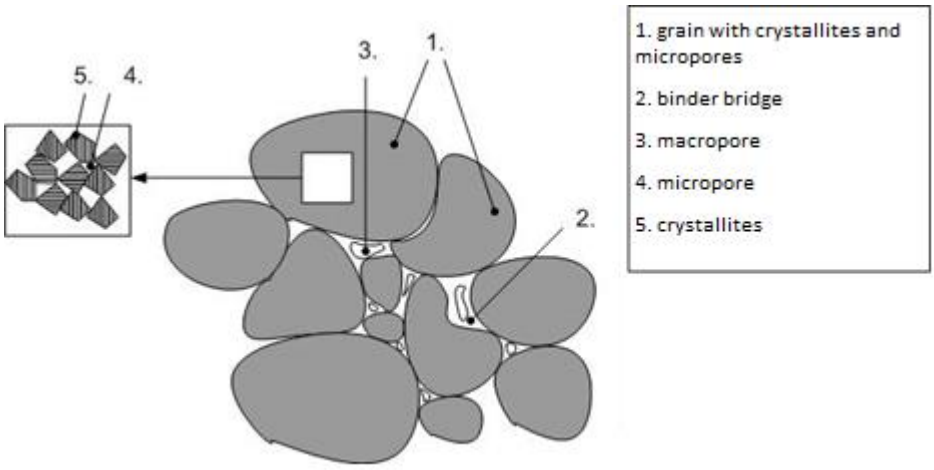


Figure 2.2: Polycrystalline graphite mold [DEL83]

Macro- and mesopores (3. in Figure 2.2) originate in the binder between the coke grains because of bubbling during the pyrolysis. The gas produced during pyrolysis escapes from the binder and builds ducts throughout the mold which will become porosities after cooling.

In addition the coke grains get porous by the same mechanism. Micropores are formed mainly between the crystallites parallel to the lattice plane.

The porosity of fine grain graphites is between 15 to 20 % depending on type and amount of binders.

Reactor graphites were used at Research Center Jülich in different research reactors:

FRJ-1 Merlin, FRJ-2 DIDO and AVR.

2.1.1 Research Reactor FRJ-1 Merlin

FRJ-1 was a light-water research reactor of the pool type at Forschungszentrum Jülich with a maximum thermal power of 10 MW. It reached criticality in 1968, was shut down in 1985 and fully dismantled between 1995 and 2009 [FZJ1].

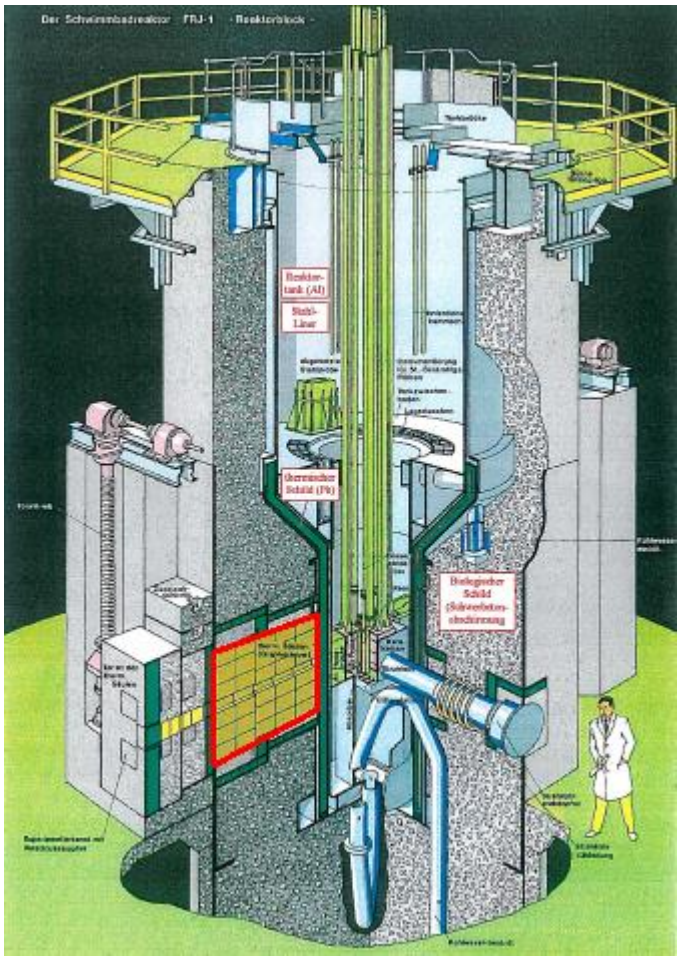


Figure 2.3: Scheme of FRJ-1 Merlin

The nuclear graphite was used in the thermal column (red marks) (see Figure 2.3).

2.1.2 Research reactor FRJ-2 DIDO

FRJ-2 was a heavy water moderated and cooled research reactor with a maximum thermal power of 23 MW. It was the partner reactor of FRJ-1 Merlin but was operated from 1968 till the year 2006. The dismantling of FRJ-2 began in late 2012 [FZJ2] [FZJ3].

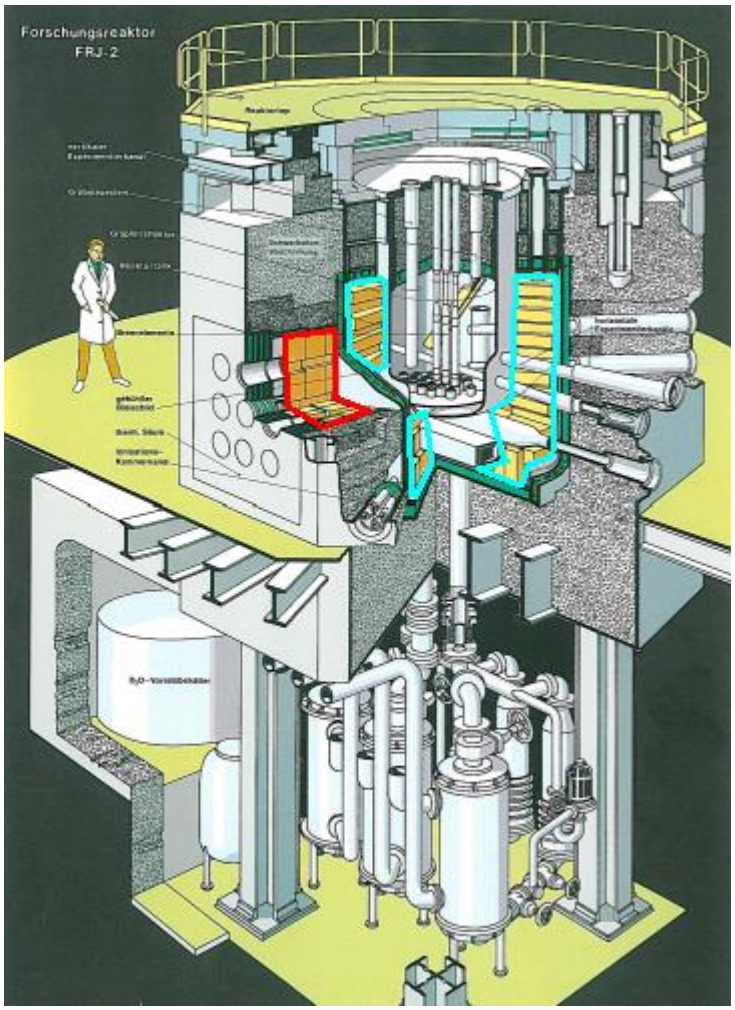


Figure 2.4: Scheme of FRJ-2 DIDO

In this reactor nuclear graphite was used as a reflector (blue marks) and in the thermal column (red marks) (see Figure 2.4).

2.1.3 High-temperature nuclear reactors

Nearly 85 % of all nuclear power plants worldwide are light-water reactors. The high-temperature nuclear reactors were developed because they can have a higher thermodynamic efficiency than light-water reactors [KUG89].

The reactor AVR was used to explore high-temperature reactor designs as realized, e.g. in the THTR-300 where reactor-grade graphite was used to a large extent.

The pebble bed nuclear reactor was developed as a very high temperature reactor of generation IV nuclear reactors. The pebble bed reactors in Germany are AVR in Jülich and THTR-300 in Hamm-Uentrop.

In a pebble bed reactor helium is used as coolant and graphite as construction material, moderator and reflector. Graphite was used because of its capability to absorb a part of the energy of fast neutrons, when they collide with carbon atoms in the graphite lattice.

In addition, the core was surrounded by so called carbon brick, a lower quality graphitic material.

Specific for a pebble bed reactor is the use of spherical coated particles containing nuclear fuel as UO_2 and ThO_2 coated with SiC and pyrocarbon. The diameter of such a sphere is ≈ 6 cm and of the fuel particles is around 0.5 mm.

The core of the reactor is covered with a graphite reflector of 0.5 m width [FIS12].

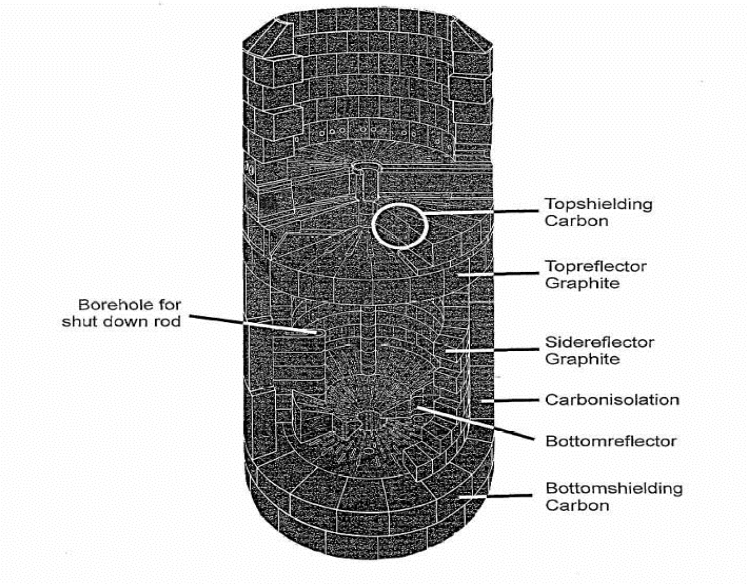


Figure 2.5: AVR graphite and carbon installations [POD04]

2.1.4 Gas –cooled reactors

EDF (Electricite De France) operated in France six gas-cooled reactors, all shutdown now for at least fifteen years. These reactors are of so-called in French, “UNGG” reactor type (Uranium Naturel Graphite Gaz). They were graphite moderated, cooled by carbon dioxide and fuelled with natural metallic uranium.

The Saint-Laurent A2 (SLA2) reactor was commissioned in August 1971. The pressure vessel of this reactor is built of prestressed concrete which also acts as biological shielding. The coolant is CO_2 which circulates from top to bottom at a pressure of 29 bar in the space between the graphite and the Mg-Zr alloy fuel cladding. The operating temperature ranges between 240°C (top) and 470°C (bottom). The thermal power is 1,700 MW. The gross electrical power is 530 MWe and the net electrical power in nominal operation is 515 MWe. The thermal neutron flux (from 10^{-5} eV to 0.5 eV) in the central zone of the core and in the maximum flux plane is 3.12 10^{13} $n.cm^{-2}.s^{-1}$.
It should also be noted that this reactor was shut down between March 1980 and September 1982 following an incident which led to the melting of two fuel elements at the bottom of the F5 M19 C14 channel (loss of cooling of the channel as a result of its obstruction by a metal plate, leading to overheating of the fuel elements).
The SLA2 reactor was finally shutdown on May 25, 1992. It was operated during 11 years full equivalent operating power. It has been defuelled and has been placed in a safe enclosure mode (ventilated by air with a moisture content limited to 50 %) until the final dismantling is performed.
EDF received the authorization to fully dismantle the SLA2 reactor by decree 2012-510 of May 18, 2010. All non nuclear parts of SLA2 nuclear unit have been dismantled (dismantling IAEA level II achieved - figure 2). Up to now, final dismantling (level III) is planned by 2030-2040.



Figure 2: Saint-Laurent A1 (left) and Saint-Laurent A2 (right)

The graphite stack of the SLA2 reactor has the form of a cylinder with a vertical axis 15.73 metres in diameter (13.43 metres of moderator surrounded by a 1.15 m thick reflector) and 10.2 metres high. The total mass of graphite is 2,440 tons including 1,580 tons of moderator and 860 tons of reflector (figure 3).

The stack's network of graphite bricks is a hexagonal mesh with a pitch of 225.16 mm. The elementary graphite blocks are prismatic bars with a hexagonal base whose distance between two opposite faces is equivalent to the network mesh. The side-by-side juxtaposition of 4,429 bars forms a bed, the SLA2 stack consisting of 8 superimposed beds (bed No. 1 is that at the bottom of the stack). Thus, the bars are superimposed and the stack may also be regarded as the juxtaposition of 4,429 columns. The graphite stack comprises:

The lateral reflector consisting only of 828 solid columns surrounding the core;

The moderator (or core) consisting of 3,601 columns: 345 solid columns, 181 bored to 84 mm for the control rods and 3,075 columns bored to 140 mm (basically for the fuel elements).

2.2 Graphite as nuclear waste

During operation reactor graphites are irradiated and acquire radioactive materials. Most activity of graphite molds arises from the neutron induced reactions of carbon, ^{3}H and other activation of stable impurities. The main issue with ^{14}C is its half-life of 5730 years and very high bio-compatibility; therefore it is necessary to keep ^{14}C away from the biosphere, where it could contaminate plants, animals and other life forms. ^{3}H has a half-life of 12.32 years and is also a hazard to the biosphere because of a very quick isotope exchange reaction.

2.2.1 Carbon-14

Carbon - 14 is created in the following nuclear reactions:

- ^{13}C (n, γ) ^{14}C
- ^{14}N (n, p) ^{14}C
- ^{17}O (n, α) ^{14}C

Most of ^{14}C (> 99 %) is formed by the reaction ^{14}N (n, p) ^{14}C.
Nitrogen is an impurity within the graphite mold. Graphite has the ability to adsorb nitrogen onto the boundary layer. Other nitrogen impurities are results of the production process and these impurities normally are embedded in porosities.

2.2.2 Tritium

Tritium (^{3}H / T) is mostly produced by the following nuclear reactions:

- ^{235}U (n, f) ^{3}H
- ^{6}Li (n, α) ^{3}H
- ^{3}He (n, p) ^{3}H
- ^{10}B (n, 2α) ^{3}H
- ^{14}N (n, T) ^{12}C

^{3}H is an isotope of ^{1}H and quickly exchanges with stable hydrogen in a water molecule:

$$HT + H_2O \rightarrow HTO + H_2$$

This reaction is utilized to trap and analyze the ^{3}H content of the i-graphite.

2.2.3 Other radionuclides

Caesium

Nuclear fission and neutron capture reactions are producing radioactive caesium isotopes ^{134}Cs, ^{135}Cs and ^{137}Cs:

- $^{235}U \rightarrow {}^{137}Cs, {}^{135}Cs$
- $^{235}U \rightarrow {}^{133}Cs\ (n, \gamma)\ {}^{134}Cs$

Impurities of ^{133}Cs can also be a source of ^{134}Cs:

- $^{133}Cs\ (n, \gamma)\ {}^{134}Cs$

The half-lives of these isotopes are:

- ^{134}Cs: 2 years
- ^{135}Cs: 2 E+06 years
- ^{137}Cs: 30.1 years

The sources of these caesium-contaminations are, as mentioned above, both impurities within the nuclear graphite or uranium [POD04].

Europium

The europium isotopes ^{152}Eu, ^{154}Eu and ^{155}Eu are both products of fission reactions and activation of impurities of ^{151}Eu, ^{153}Eu and ^{154}Sm [POD04].
The half-lives of these isotopes are:

- ^{152}Eu: 12.4 years
- ^{154}Eu: 8.5 years
- ^{155}Eu: 4.5 years

Cobalt

The stable ^{59}Co produces ^{60}Co by neutron activation. ^{59}Co is present as an impurity in nuclear graphite [POD04]. ^{60}Co has a half-life of 5.3 years.

2.2.4 Activity inventory

The following tables (Table 2.1, Table 2.2) show that concentration of radioactive materials and amount of activity is significant. Therefore AVR graphite is considered radioactive waste [POD04].

Another problem emerges in the disposal of contaminated graphite materials, because the ^{14}C activity of graphite reflectors would amount to more than 90 % of the total ^{14}C activity licensed for the underground disposal site Konrad in Germany for non-heat-generating radioactive waste [FAC08].

Concentration [ppm]		
Carbon brick	**Reflector**	**Activation product**
30	2	^{3}H
10	2	^{3}H
990,000	1,000,000	^{14}C
4,500	30	^{14}C
15	0.2	^{36}Cl
1,600	30	^{40}K
1,500	100	^{41}Ca
7,000	1,000	^{55}Fe
10	0.2	^{60}Co
40	10	^{63}Ni
2.5	0.05	^{94}Nb
10	2	^{93}Mo, ^{99}Tc
1	0.01	^{134}Cs
100	20	^{133}Ba
2	0.02	^{151}Sm, ^{155}Eu
0.1	0.02	^{152}Eu, ^{154}Eu

Table 2.1: Impurities of AVR graphites [POD04]

Radionuclides	Activity [Bq]	
	Carbon brick	Reflector
^{3}H	6.9 E+15	8.8 E+14
^{14}C	2.9 E+14	4.6 E+12
^{36}Cl	5.9 E+10	1.5 E+09
^{41}Ca	4.5 E+11	5.8 E+10
^{55}Fe	4.0 E+15	1.1 E+15
^{60}Co	1.1 E+15	4.2 E+13
^{63}Ni	8.5 E+12	4.1 E+12
^{93}Mo	4.1 E+08	2.5 E+08
^{99}Tc	3.5 E+07	2.8 E+07
^{134}Cs	3.1 E+13	8.9 E+11
^{133}Ba	7.1 E+11	3.5 E+11
^{151}Sm	1.8 E+10	4.5 E+08
^{152}Eu	2.9 E+07	1.4 E+07
^{154}Eu	3.0 E+11	1.5 E+11
^{155}Eu	2.5 E+12	6.3 E+10
^{166m}Ho	4.3 E+10	2.2 E+09

Table 2.2: Total activity of AVR graphites [POD04] [FIS12]

2.2.5 Disposal of irradiated reactor graphites

In general, the objective of a nuclear waste repository is secure long-term disposal without contact to the biosphere. In Germany, nuclear wastes will be disposed in underground rock formations or salt mines. As many radionuclides have long half-lives ranging from some hundred to millions of years it is necessary to develop a secure repository strategy in order to minimize the transport of radioactive materials to the biosphere. This idea utilizes a multi-barrier system of natural and technical origin, like clay stratums and special containers designed for final repository to seal radionuclides from the biosphere.

Presently, there are four final repositories and final repository projects in Germany:

- Asse repository (existing)
- Morsleben repository (existing)
- Konrad repository (projected)
- Gorleben exploratory mine.

While Gorleben is an exploratory mine and it remains unclear whether radioactive waste will be terminally stored there, Morsleben and Asse already have stores of radioactive waste. The Konrad mine is currently converted into a repository. In compliance with the Atomic Energy Act and current mining legislation, the Federal Office for Radiation Protection (BfS) assumes sole responsibility for operations at the Gorleben and Konrad mines and for the decommissioning of the Morsleben and Asse repositories.

Furthermore, nuclear waste is divided in two categories:

- The first category is heat-generating nuclear waste. Spent nuclear fuel elements and liquid high-level radioactive waste falls into this category.
- The second category is nuclear waste with negligible heat generation. This category contains mostly other primary waste like cleaning cloth, disused tools and plant, used filters or residues from waste water treatment [BfS].

The i-graphite used in nuclear reactors falls into the second category.
The current strategy is a volume-optimized storage in Konrad repository and the irradiated graphite would consume a huge amount of the available space in the repository.
Therefore, separation of ^{14}C from ^{12}C would be a valuable solution to minimize the volume of waste.

2.3 Decontamination procedures for irradiated nuclear graphite

2.3.1 Treatment processes

The decontamination processes for irradiated nuclear graphite are still experimental. The most common idea for a treatment process is the thermal treatment of graphite.
The burning of irradiated graphite would be an efficient method for volume reduction, but is not an option because ^{14}C would be emitted into the atmosphere in form of CO_2.
Therefore pyrolyzing graphite in inert or light oxidizing conditions is better way to separate ^{14}C from ^{12}C [FAC08].
Currently, there are a few thermal treatment processes at Research Center Jülich FZJ.
These processes use a variety of atmospheres, temperature and duration for the graphite treatment.
The atmospheres used for the treatment experiments were:

- inert atmospheres: N_2, Ar
- light oxidizing atmospheres: N_2 + 0.1 % to 1 % O_2, Ar + H_2O

The temperature used range from 750 °C to 1300 °C and the duration of isothermal treatment from 4 to a maximum of 40 hours (see A.2).
Because of these experiments, reforming of graphite with steam is supposed to be a valid way to separate ^{14}C from ^{12}C without a mass loss over 10 %.

2.3.2 Steam reactions with graphite solid bodies

When steam reacts with carbon, carbon monoxide and hydrogen are formed (steam reforming):

$$C + H_2O \rightarrow CO + H_2$$

The secondary reactions of the steam reforming process are:

$$CO + H_2O \rightarrow CO2 + H_2$$

$$C + 2H_2 \rightarrow CH_4$$

$$2CO \rightarrow C + CO_2$$

Another reaction taking place is the oxidation of CO to CO_2 with the help of CuO:

$$CuO + CO \rightarrow CO2 + Cu$$

These reactions results in the formation of gaseous CO_2, which can be washed out of the gas flow easily by using the following reaction:

$$CO_2 + NaOH \rightarrow Na_2CO_3 + H_2O$$

^{14}C is expected predominantly to reside between graphite layers and not bounded within them. Therefore one anticipates extracting a large fraction of ^{14}C by this process.
In order to perform this steam reformation with i-graphites, steam has to reach into the graphite and the CO_2 formed to escape.
Such gas transport mechanisms are typically described as diffusion processes according to Fick's laws:

$$J = \frac{1}{A}\frac{dN}{dt} = -D\frac{\partial c}{\partial x}$$

$$\frac{dc}{dt} = D\frac{\partial^2 c}{\partial x^2}$$

The first law describes the flow, which passes through an area A in a unit of time. The second law describes in a differential equation a time-dependent change of concentration of a gas diffusing in a solid body. The diffusion constant D can also be a unit to measure the speed of the change of concentration.
The porous solid body is subject to different corrosion behaviors depending on temperature as shown in figure 2.6.

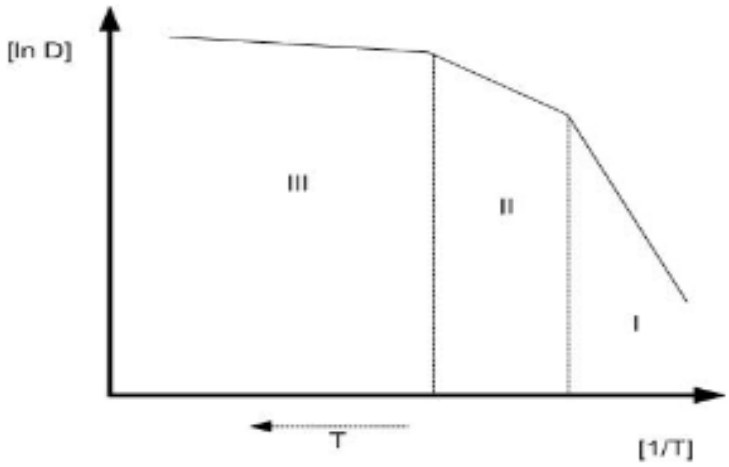


Figure 2.6: Arrhenius diagram of corrosion ranges [FIS12]

Part I has a temperature range of $\vartheta < 800$ °C and is called *chemical range*. The steam diffuses into the porosities and reacts with the whole surface of these porosities (see Figure 2.7). Due to the slow reaction speed there is no change in concentration within the graphite [DEL83].

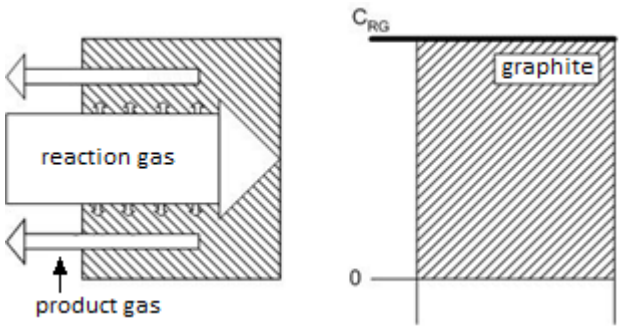


Figure 2.7: Diagram of chemical reaction and concentration trend of reaction gas [FIS12]

Part II has a temperature range of 800 °C $< \vartheta <$ 1250 °C and is called *pore diffusion range.* The reaction speed of graphite increases faster than the amount of available steam. Therefore the concentration of steam within graphite decreases with depth; this means the deeper layers stay intact (see Figure 2.8) [DEL83].

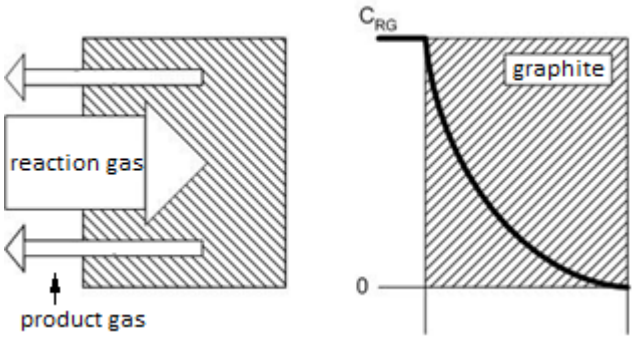


Figure 2.8: Diagram of pore diffusion and concentration trend of reaction gas [FIS12]

Part III has of temperature range of 1250 °C < ϑ < 1400 °C and is called *boundary layer diffusion range*. The steam reacts with the surface of the solid body very fast, so that is not possible for the steam to diffuse into the porosities of the graphite (see Figure 2.9).There is no reaction within the porous solid body, because of the higher temperature. The emerging CO and CO_2, respectively, arise solely from the reaction with the graphite surface [DEL83].

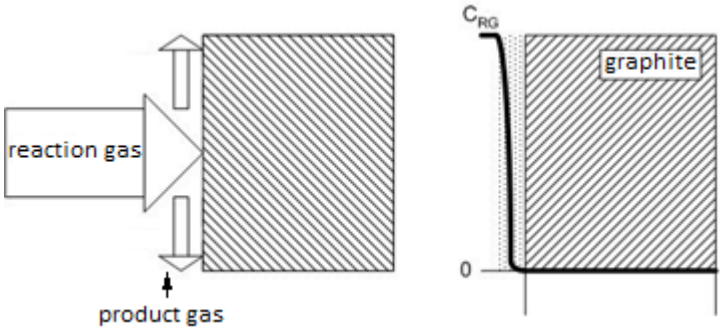


Figure 2.9: Diagram of boundary layer diffusion and concentration trend of reaction gas [FIS12]

The designated reaction of steam and graphite to decontaminate the graphite of ^{14}C and ^{3}H is taking place at temperatures above 900 °C within the pore diffusion range.

2.3.3 Determination of radionuclide release

To determine the release of ^{3}H and ^{14}C the values of the LSC measurement have to be calculated as follows:

$$cpm_{corr.} = cpm - BG$$

$$dpm = \frac{cpm_{corr.}}{\varepsilon}$$

$$A_{mL} = \frac{dpm}{60}$$

$$A_{sample} = A_{ml}\left(V_{db} - (n-1)V_{st}\right)$$

Therefore the final equation is:

$$A_{sample} = \frac{cpm - BG}{60\,\varepsilon}\left(V_{db} - (n-1)V_{st}\right)$$

- A_{mL} is activity in Bq/mL
- A_{sample} is activity in Bq/graphite-sample
- BG is background
- V_{db} is the volume of the full bubbler
- V_{st} is the volume of the taken sample from the bubbler
- ε is the efficiency of LSC measurement derived from tSIE-value
- n is the number of the taken sample

3. Material & Methods

3.1 Steam reforming installation

3.1.1 Equipment

The equipment for steam reforming experiments consists of:

- a high-temperature oven: *Carbolite STF 15/-/180*
- another oven for oxidizing CO to CO2: *Carbolite MTF 10/15/130*
- a humidity generator: *SETARAM WetSys*
- a carrier gas supply system made by *Linde*
- absorbers for ^{3}H and ^{14}C and
- for measuring ^{3}H and ^{14}C: a *Parckard Liquid Scintillation Analyzer TriCarb 2770 TR/SL*

The furnace tube is made of recrystallized alumina (99.7 % Al_2O_3) and has a size of 50 mm × 60 mm × 900 mm (inner diameter × outer diameter × length).

The pipes and junctions are made by *Swagelok*.

The "double bubblers" and the special designed sample holder are made by *Zentralinstitut für Technologie (ZAT)* at Forschungszentrum Jülich.

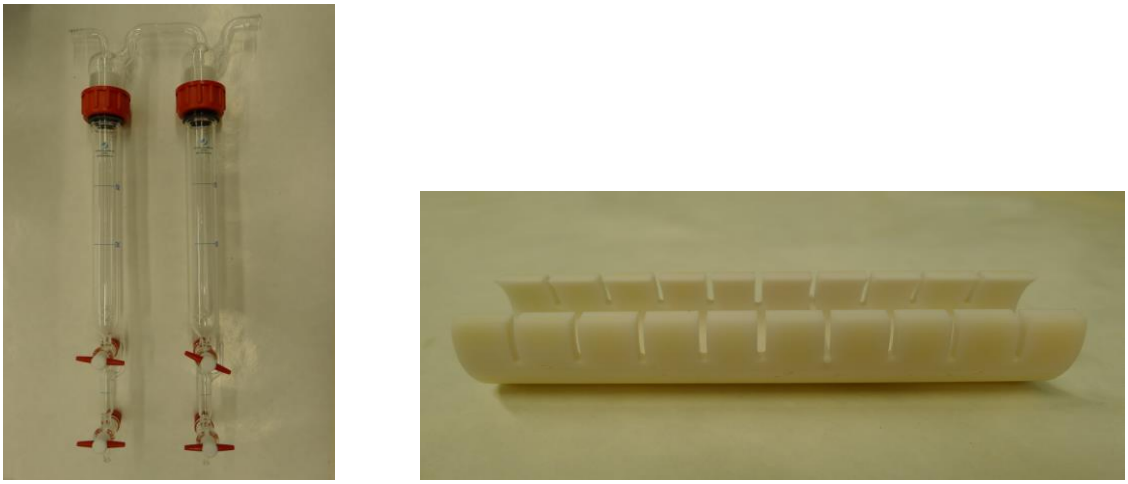


Figure 3.1: A double bubbler and a special designed sample holder made by ZAT

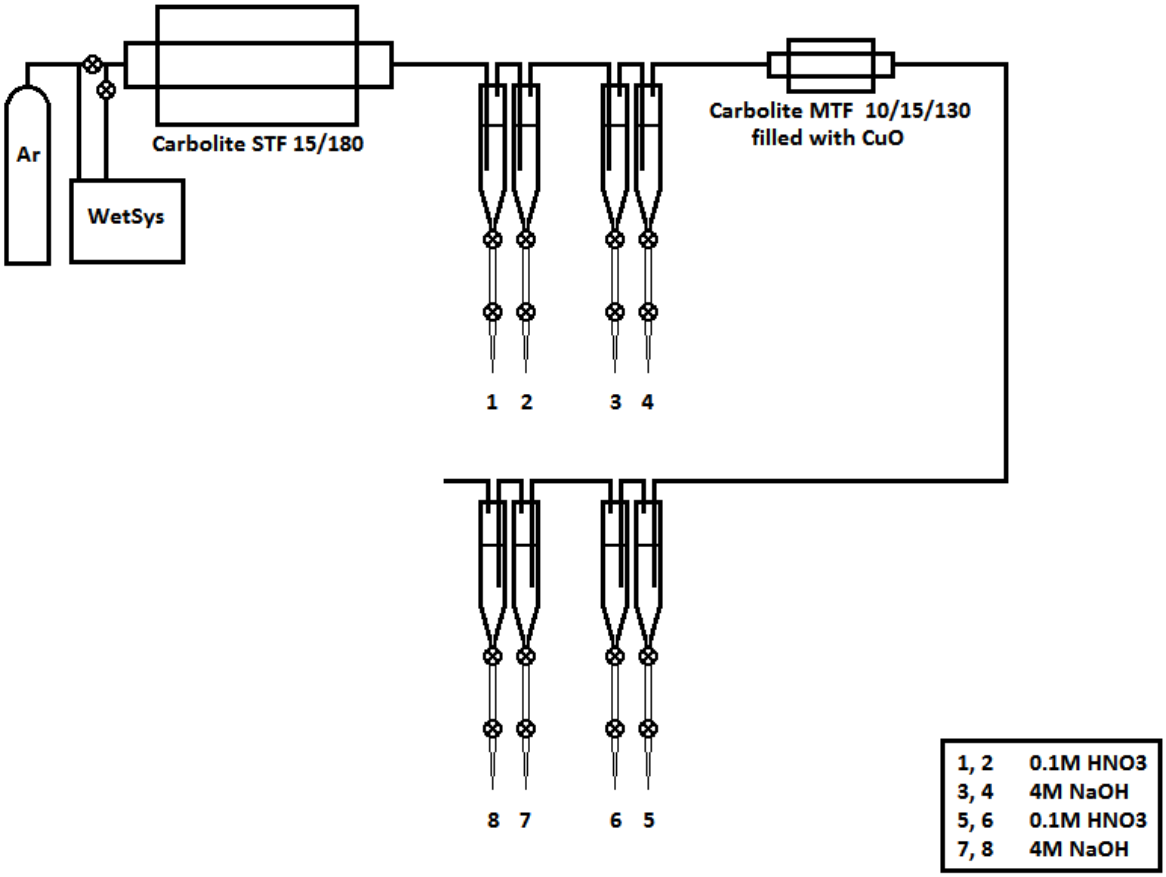


Figure 3.2: A sketch of the treatment installation

3.1.2 Reagents

Following chemicals were used during the experiments:

Sodium hydroxide	NaOH	4 M	*Merck*
Nitric acid	HNO_3	0.1 M	
Copper oxide	CuO		*Merck*
Argon	Ar	> 99.9999 %	*Praxair*
HIONIC FLUOR	LSC Cocktail		*Packard*

3.1.3 Installation description

The experimental installation for graphite decontamination consists of the Carbolite STF 15/-/180 tube furnace with a special aluminum oxide tube and the humidity generator WetSys. At the end of the tube are various “double bubblers” filled with NaOH and HNO_3 and another smaller tube furnace (Carbolite MTF 10/15/130) filled with CuO to enforce the reaction of CO to CO_2.

The WetSys is connected to the argon gas supply line. There is another gas line parallel to the WetSys connected to the furnace in front of the high quality steel flange. Both connections can be activated via gas tap.

The exit of the tube is connected to at least four ”double bubblers”. The first pair is filled with 4 M NaOH to trap redundant tritium (^3H / T) in form of THO. The second pair is filled with 0.1 M HNO_3 to trap redundant $^{14}CO_2$ in form of Na_2CO_3. The smaller tube furnace is placed behind the second double bubblers to ensure that ^{14}CO reacts to $^{14}CO_2$. The third and fourth double bubblers are placed at the exit of the tube furnace and are filled with NaOH and HNO_3 to trap the remaining ^3H and ^{14}C.

All pipes and junctions are made of components made by Swagelok, except the flange adapters which were specially made by ZAT to be compatible with Swagelok components (see Figure 3.2 for installation sketch).

3.2 Materials investigated and sample preparation

3.2.1 DIDO graphite

DIDO graphite samples are not irradiated, so called *virgin*. They have cylindrical shape with a length of 20 mm and a diameter of 8 mm. It was necessary to make a small hack into the samples to minimize the movement on the sample holder.

Before mounting them on the sample holder and inserting them into the furnace tube, the mass of all samples was taken on an analytical balance (*Mettler Toledo XS205 Dualrange*).



Figure 3.3: DIDO graphite sample

3.2.2 Irradiated Merlin graphite

Samples of Merlin graphite were cut in a glove box. They also have nearly cylindrical shape with varying length and diameter. The surface of these samples is much rougher than the DIDO graphite surface.

Before mounting them on the sample holder and inserting them into the furnace tube, the mass of all samples was taken on an analytical balance (*Mettler Toledo XS205 Dualrange*).



Figure 3.4: Merlin graphite samples

The exact specifications of the Merlin samples were:

	Merlin – 1	**Merlin – 2**	**Merlin – 3**
Length [mm]	8 – 10	8 – 11	10 – 12
Diameter [mm]	8	8	8
Weight [g]	0.6472	0.7428	1.0428
Activity of ^{3}H [Bq]	1.12 E+03	1.20 E+03	approx. 1.74 E+03
Activity of ^{14}C [Bq]	2.30 E+02	2.64 E+02	approx. 3.70 E+02

Table 3.1: Merlin graphite samples

3.2.3 Irradiated Saint Laurent Graphite

Samples of Saint Laurent (SLA) graphite were cut in a glove box. They also have nearly cylindrical shape with varying length and diameter.

The SLA samples came each from a different position of the reactor. These positions are set by the level at which the sample were taken.

…

Before mounting them on the sample holder and inserting them into the furnace tube, the mass of all samples was taken on an analytical balance (*Mettler Toledo XS205 Dualrange*).

The exact specifications of the Merlin samples were:

	SLA R1 1680	**SLA R4 5120**
Length [mm]	18	12.3+/-0.3
Diameter [mm]	8	8
Weight [g]	1.3244	0.93696
Activity of ^{3}H [Bq]	1.28 E+05	1.31 E+05
Activity of ^{14}C [Bq]	6.87 E+04	6.39 E+04

Table 3.1: SLA graphite samples

3.3 Treatment and analysis of graphite

3.3.1 Experimental parameters and treatment operations

The experiments were performed with virgin DIDO graphite, irradiated Merlin graphite and irradiated Saint Laurent graphite. As WetSys accepts only input in relative humidity (%), the desired absolute humidity has to be converted. For comparison with other work, e.g. [POD04], also partial pressures are given.

Absolute humidity [g/kg]	Relative humidity [%]	Partial pressure [kPa]
5.0	14.4	0.8
7.5	21.6	1.2
10.0	28.8	1.6
12.5	35.9	2.0
15.0	43.1	2.4
17.5	50.2	2.8

Table 3.2: WetSys parameters

The internal water tank of the WetSys is heated to 35 °C and the supply line to furnace is heated to 40 °C.
For steam reforming it is necessary to eliminate all oxidizing agents besides H_2O. Therefore the tube needs to be flushed with argon before the actual experiment can be started.

3.3.1.1 Virgin DIDO graphite

The experiments with virgin DIDO graphite are used to determine operation conditions of the setup. The use of different temperatures and levels of humidity (Table 3.2) were also necessary to know if the furnace could operate with these parameters.

The operation conditions investigated are:

- Temperatures: 900 °C, 1000 °C, 1300 °C

- Heating rate: 5 K/min
- Gas flow: 5 L/h respectively 85 mL/min
- Time on max. temperature: 2 h

The humidity levels used for virgin DIDO graphite are:

- 900 °C: 14.4 %, 28.8 %, 43.1 %
- 1000 °C: 14.4 %, 21.6 %, 28.8 %, 35.9 %, 43.1 %, 50.2 %
- 1300 °C: 14.4 %, 28.8 %, 43.1 %

The furnace tube needs to be completely flushed with argon before the heating starts; the flushing takes about 1.5 h with a flow of 5 L/h. With the beginning of the heating the gas supply is changed to WetSys.

3.3.1.2 Merlin graphite

Based on the experiments with virgin DIDO graphite, irradiated Merlin graphite is used to determine decontamination factors with a humidity of 10.0 g/kg (1.6 kPa). Three samples were processed with the same parameters.

- Temperature: 1000 °C
- Heating rate: 5 K/min
- Gas flow: approx. 2 L/h (Ar), 25 mL/min (Ar/H_2O)
- Time on max. temperature: 4 h

The humidity level used for Merlin graphite is: 28.8 %.

The furnace is heating up only with argon until it reaches the final temperature of 1000 °C. Then the gas supply line is changed to WetSys to let the furnace operate isothermally with steam. After 4 h of isothermal operation the gas supply line is switched back to argon.

Since it was not possible to determine the end of release with a treatment time of 4 h, a second set of treatment of the samples Merlin-2 and Merlin-3 were performed for a treatment time of 6 h.

In addition when running the second set of experiments with Merlin-3 a mass spectrometer (*InProcessInstruments GAM2000*) was connected to the exhaust line of the tube furnace to gather additional data.

3.3.1.3 Saint Laurent graphite

Based on the experiments with irradiated Merlin graphite, irradiated Saint Laurent (SLA) graphite is used to determine decontamination factors with a humidity of 10.0 g/kg (1.6 kPa). Two samples were processed with the same parameters.

- Temperature: 1000 °C
- Heating rate: 5 K/min
- Gas flow: approx. 2 L/h (Ar), 60 mL/min (Ar/H_2O)
- Time on max. temperature: 10 h

The humidity level used for SLA graphite is: 28.8 %.

Before starting the experiment, the atmosphere was flushed by dry Ar gas and controlled by a mass spectrometer.

Unlike the experiments with Merlin graphite, SLA graphite is heated up from the beginning with steam till 1000 °C. The reason for the change was the mass spectrometer (*InProcess Instruments GAM2000*) that was connected to the exhaust line in order to see the beginning of the water gas reaction and gather further information's about the steam process.

Since the previous experiments showed that longer operation time increases the release of ^{14}C. The heating switched off after 10 h of isothermal operation and the oven cooled down to room temperature.

3.3.2 Liquid scintillation counting

Liquid scintillation counting is a method to determine the activity of beta emitters quantitatively.

The samples need to be dissolved or suspended in a special “scintillation-cocktail” containing an organic solvent and scintillators. Therefore a 1 mL sample of the double bubblers and 1 mL deionized H_2O are mixed with 18 mL *HIONIC FLUOR* LSC cocktail.

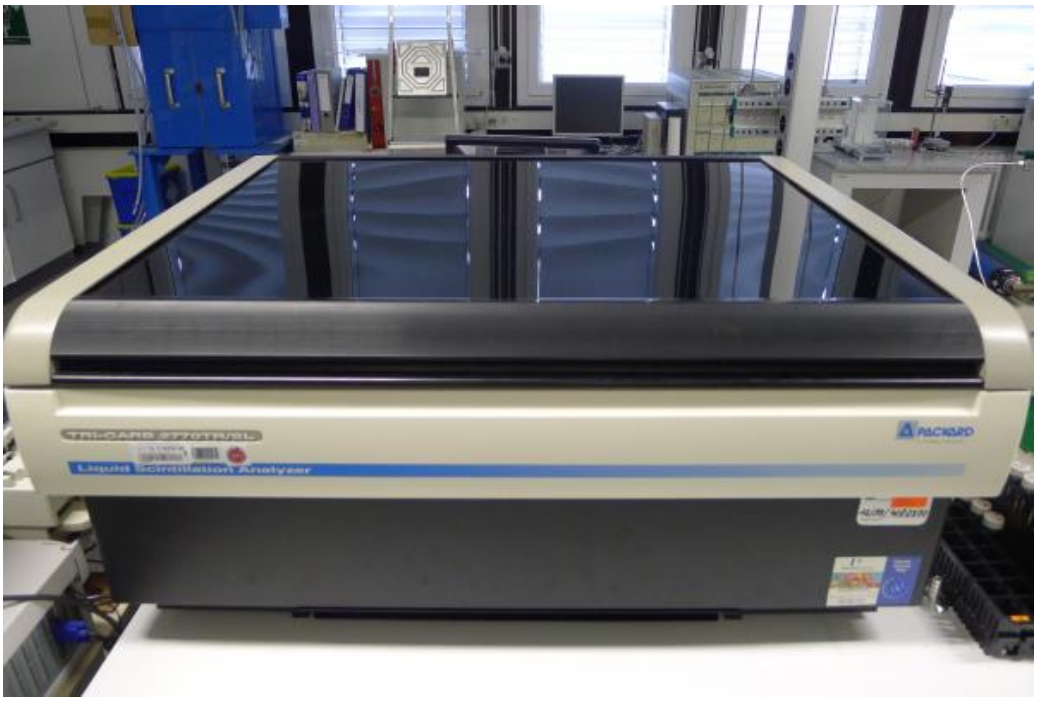


Figure 3.5: Packard Liquid Scintillation Analyzer Tri-Carb 2770 TR/SL

4. Results

4.1 System test

First tests with the tube furnace have shown that it is nearly impermeable to gases, even over long periods of time. This impermeability is important to achieve a closed system. Furthermore the Swagelok stainless steel pipes ensure the impermeability concerning the piping.

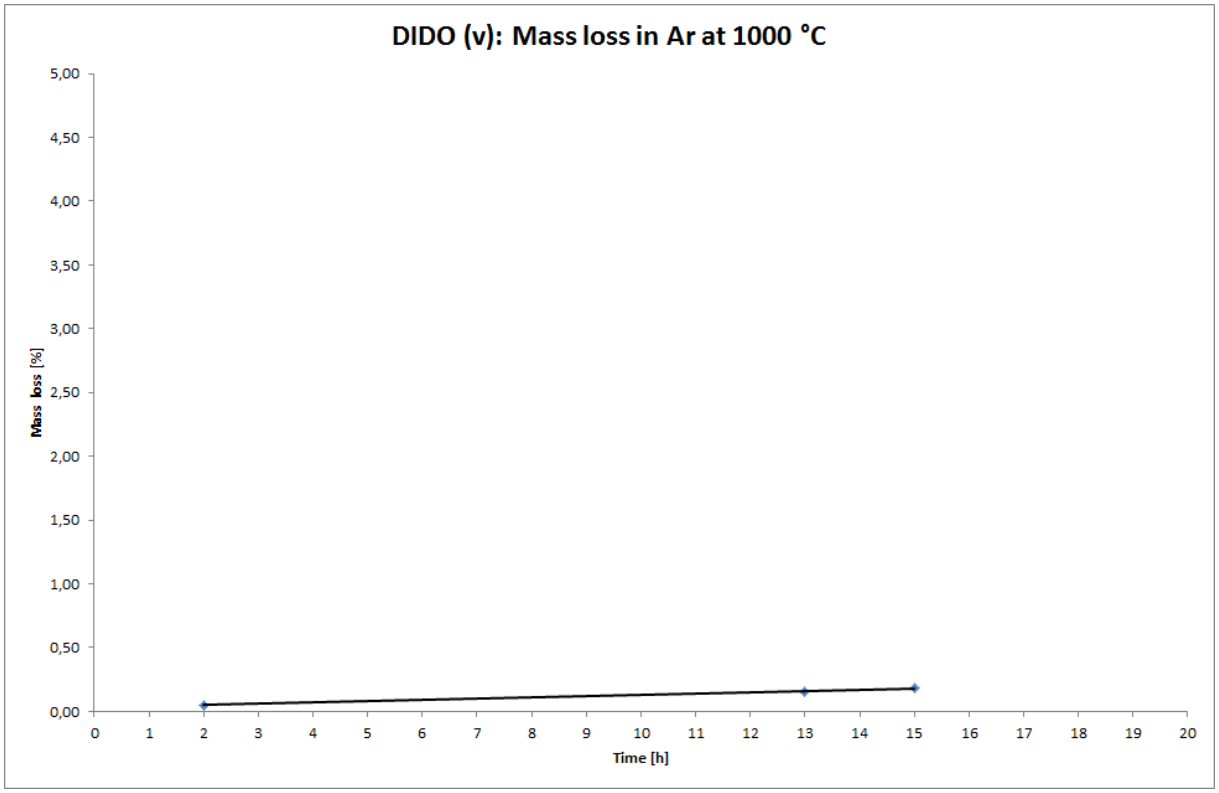


Figure 4.1: Mass loss of DIDO graphite over time

The graph illustrates the very low mass loss over time. The difference in mass loss between 2 h and 15 h of treatment in pure Ar at 1000 °C is just about 0.1 percentage points. This is also indicating that the furnace tube contains the inert atmosphere within.

4.2 Experiments with virgin DIDO graphite

The main task of these experiments was to generate reference data to indicate what parameters should be used with i-graphite. The experiments were all performed with the Carbolite STF 15/-/180 tube furnace, but without bubblers, since there were no radionuclides to trap. As mentioned before (see Chapter 3.3.1), different levels humidity and temperature were used to find suitable operation parameters.

The test series with 900 °C have too low mass losses and with 1300 °C too high mass losses. The test series with 1000 °C have the most suitable mass losses for the desired decontamination.

Furthermore the WetSys parameter of 28.8 % relative humidity, which is 10 g/kg absolute humidity, has served for the tests for irradiated nuclear graphite decontamination.

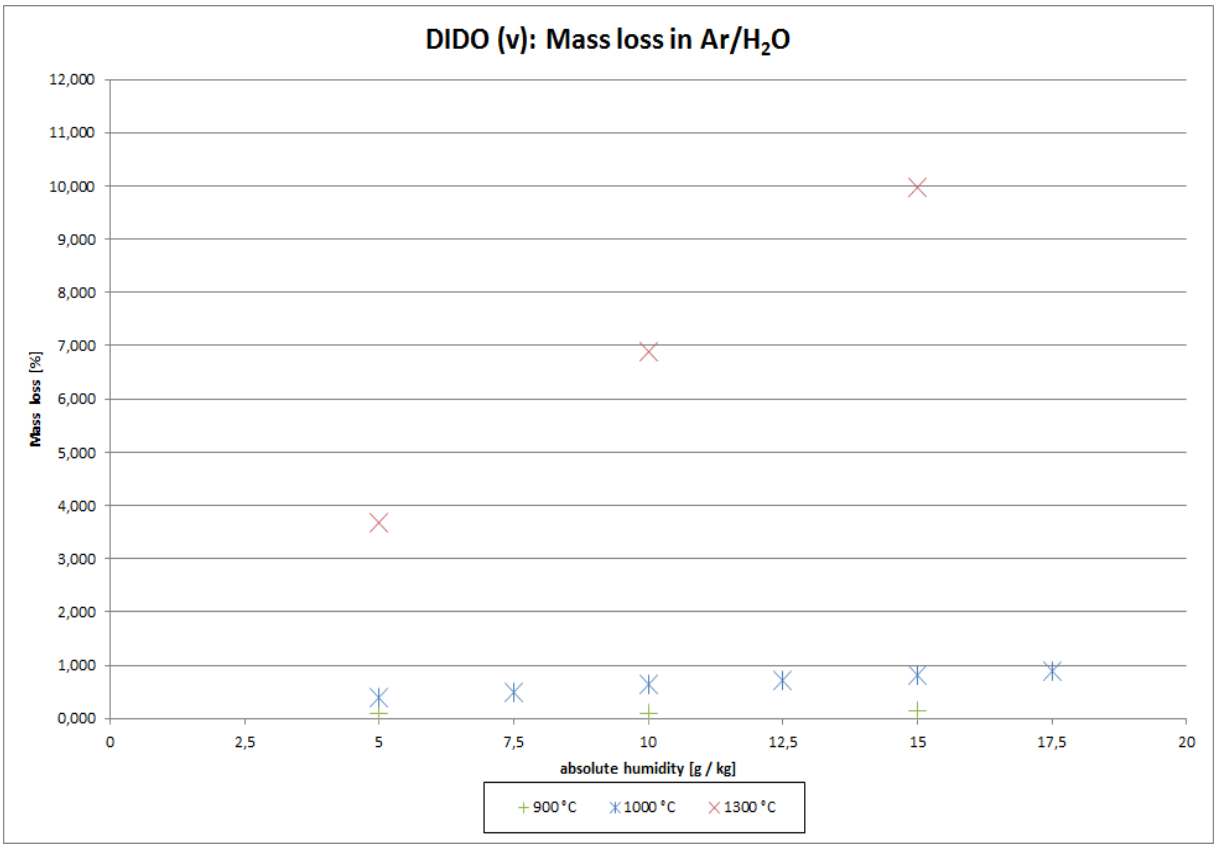


Figure 4.2: Mass loss of DIDO graphite at different temperatures

4.3 Experiments with irradiated Merlin graphite

The thermal treatment experiments with steam as oxidizing agent were performed with Merlin graphite samples described in the previous chapter.
According to previous work of [POD04] it is anticipated that the oxidation rate of ^{12}C is much higher than the release rates of radionuclides, especially ^{14}C and ^{3}H, but the fractional release of these radionuclides is higher than the fractional release of ^{12}C.

4.3.1 Performance of experiments

The first set of steam reforming treatments of Merlin-1 and Merlin-2 were performed without leakage. Regarding Merlin-3 there was a bubbler leakage at the beginning of the experiment, so there is no data for this bubbler.
In the second set of treatment of Merlin-3 there was an uncontrolled gas leakage, which made it impossible to determine the released radionuclides and therefore the original content of radioactivity. The following data of Merlin-3 are estimated.

4.3.2 Release of carbon-14

The release of ^{14}C begins around 600 °C at low rates because of the absence of oxidizing agents. At 1000 °C the oxidizing agent H_2O increases the release of ^{14}C by a great degree. The release of ^{14}C differs in the first treatment steps: the Merlin-1 sample released an amount of 20.1 % ^{14}C after the first treatment, the Merlin-2 sample just released an amount of 11.0 % and Merlin-3 released an amount of 15.0 %.
It could be possible that the Merlin-1 sample had a higher concentration of ^{14}C on the surface or near it, or it was a higher amount of O_2 present in the tube.

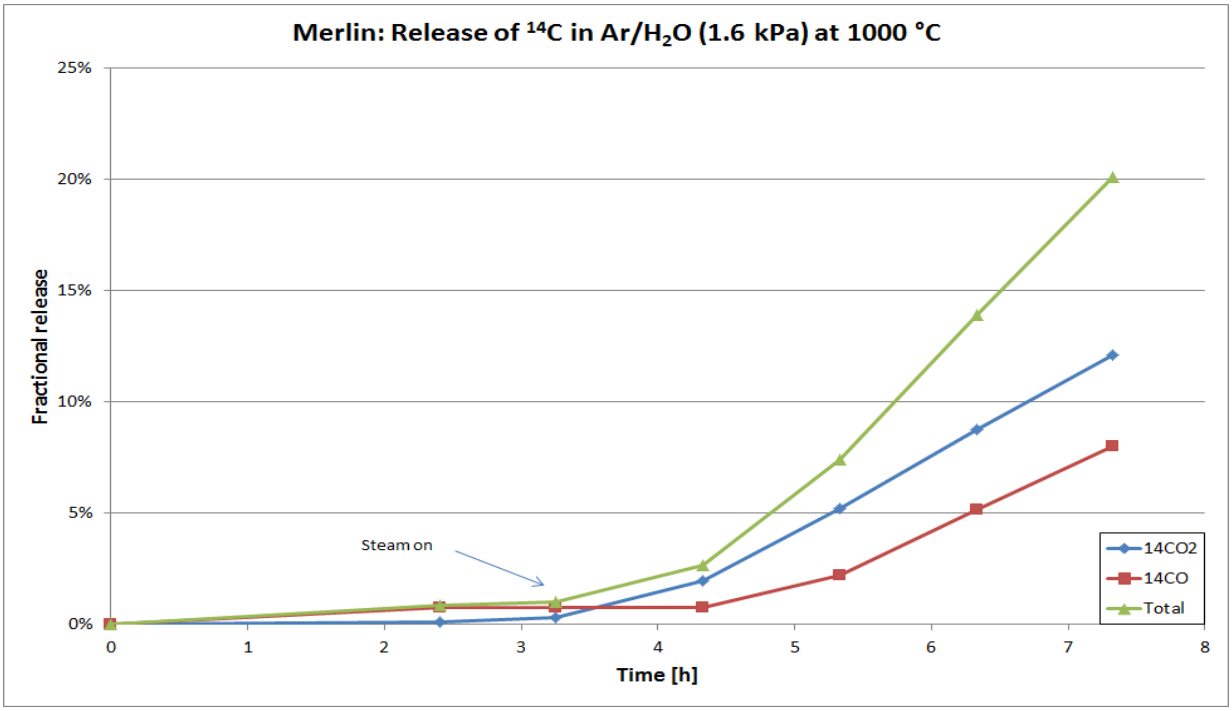


Figure 4.3: Release of ^{14}C of Merlin-1 sample

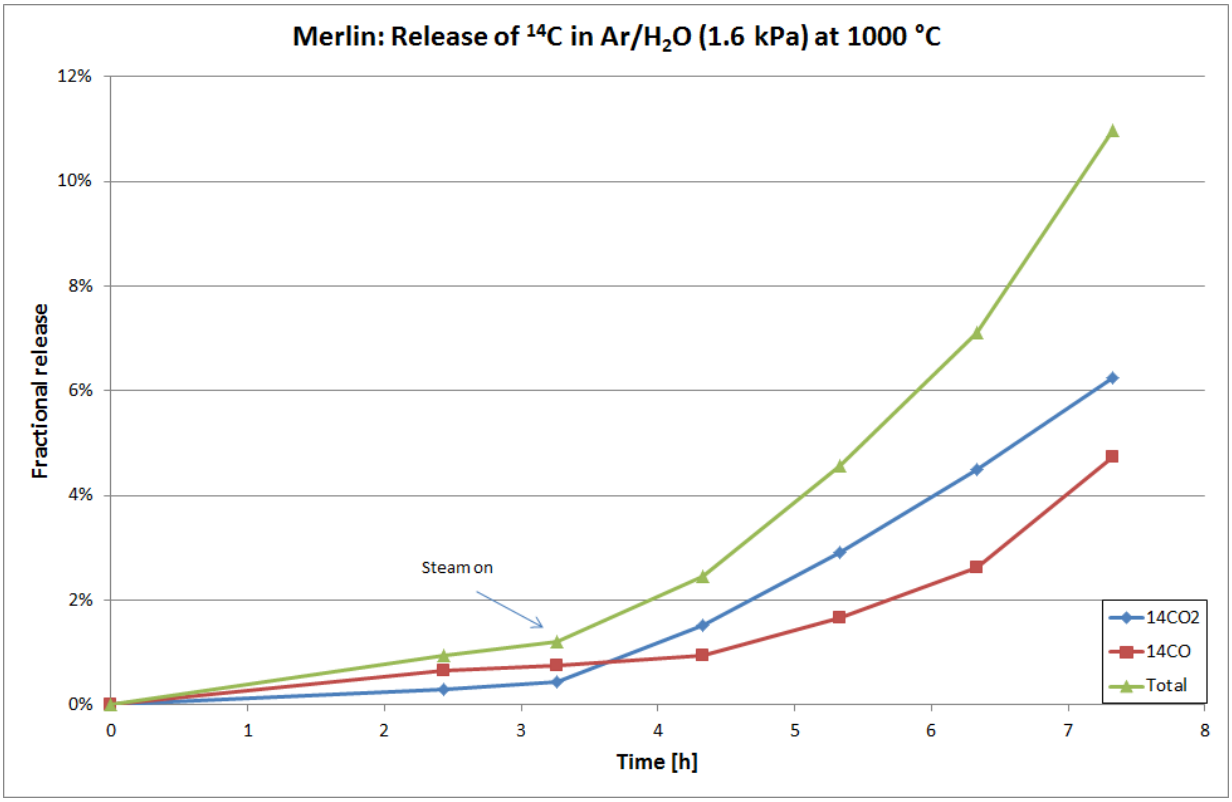


Figure 4.4: Release of ^{14}C of Merlin-2 sample

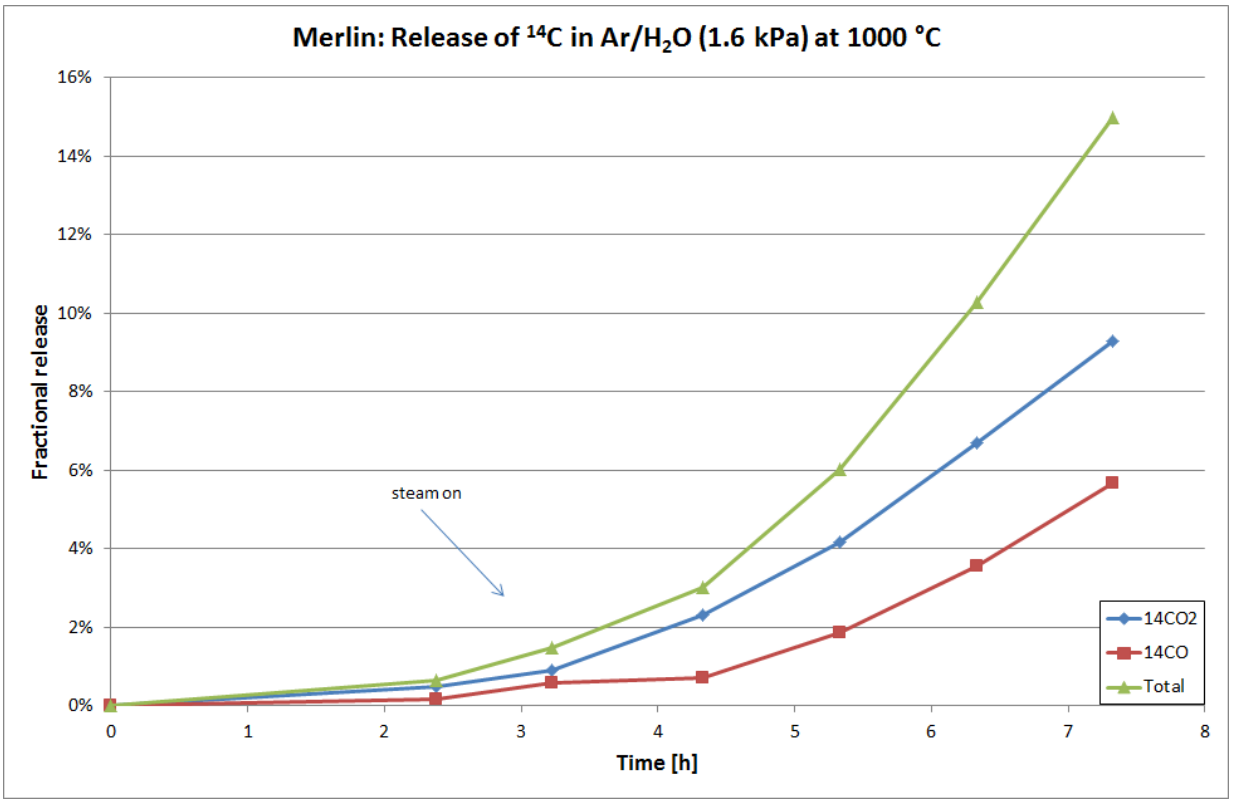


Figure 4.5: Estimated release of ^{14}C of Merlin-3 sample

As mentioned before, it was not possible to determine an end of release of ^{14}C after the first treatment of 4 h. Therefore a second set of treatment performed with Merlin-2 sample and Merlin-3 sample.

The released amount of ^{14}C of Merlin-2 raised to 18.1 % in the second treatment, totaling 29.1 % of release.

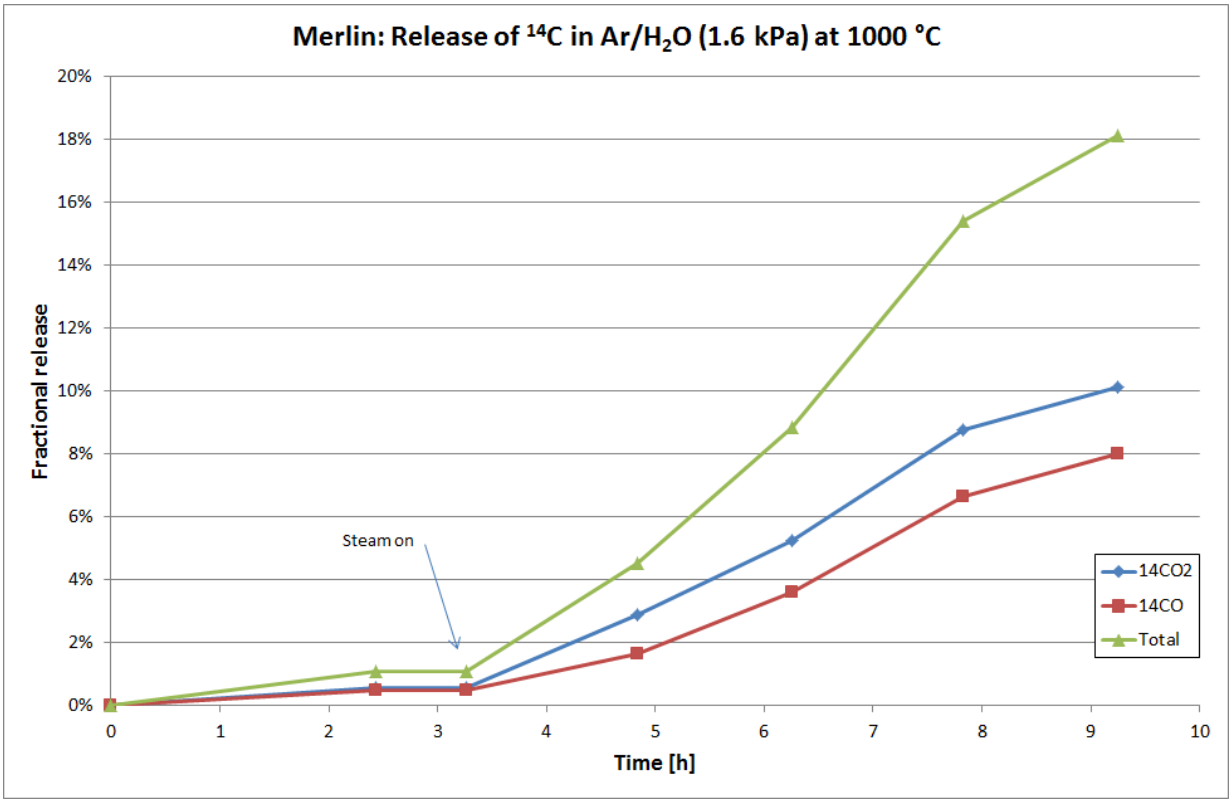


Figure 4.6: Release of ^{14}C of Merlin-2 in the second treatment

The higher release of ^{14}C could be explained with corrosion by the first treatment, creating a better surface for the steam reaction.

4.3.3 Release of tritium

The release rates of tritium do not differ as much as with ^{14}C. In the experiments with Merlin-1 and Merlin-2 the release rates were about 75 %. Merlin-3 had a lower release rate. Merlin-1 had a release of 73.3 %, Merlin-2 had a release of 77.4 % and Merlin-3 had an estimated release of 65.5 %.

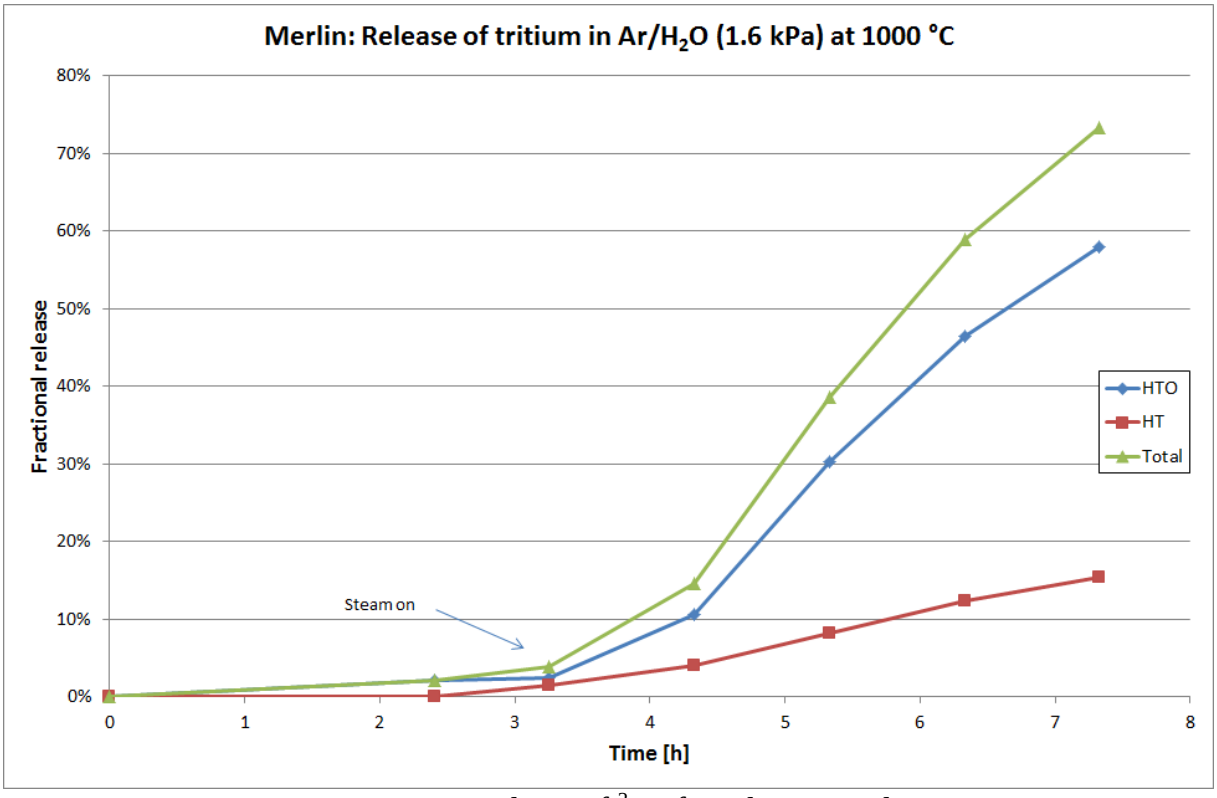


Figure 4.7: Release of ^{3}H of Merlin-1 sample

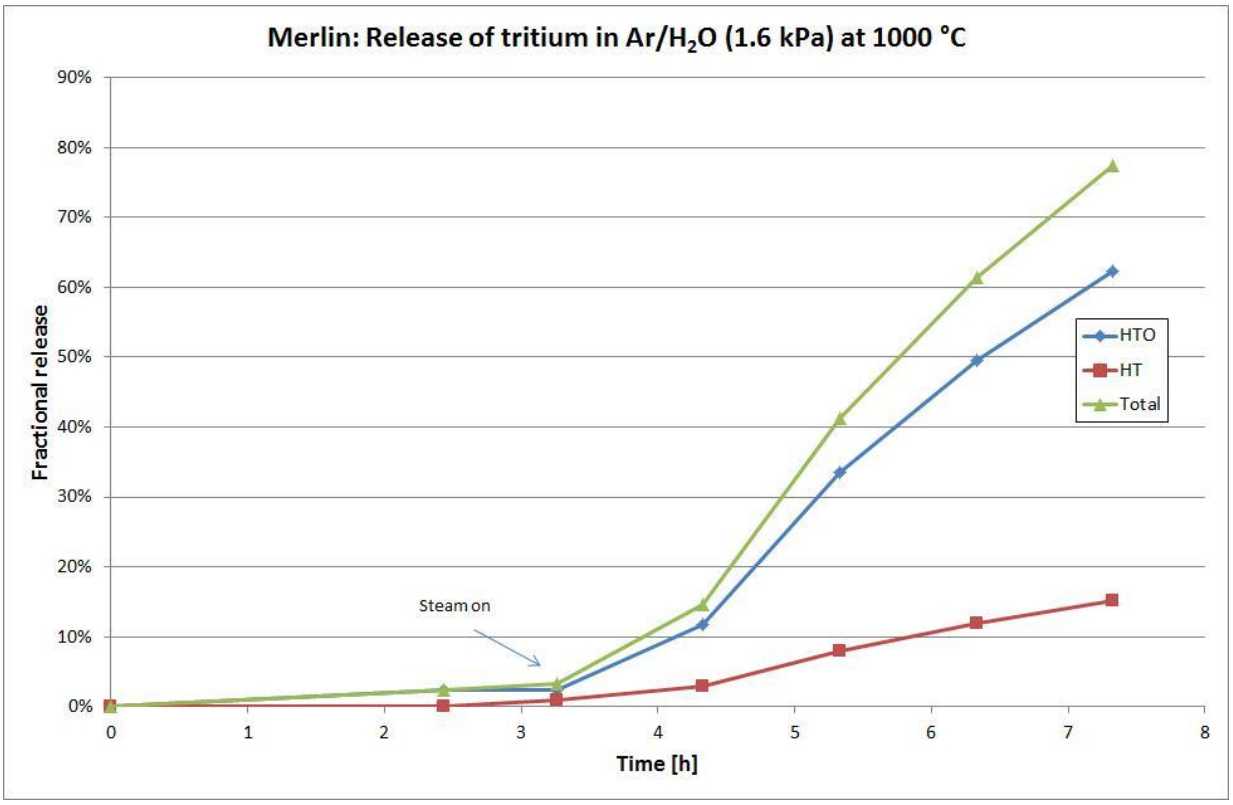


Figure 4.8: Release of ^{3}H of Merlin-2 sample

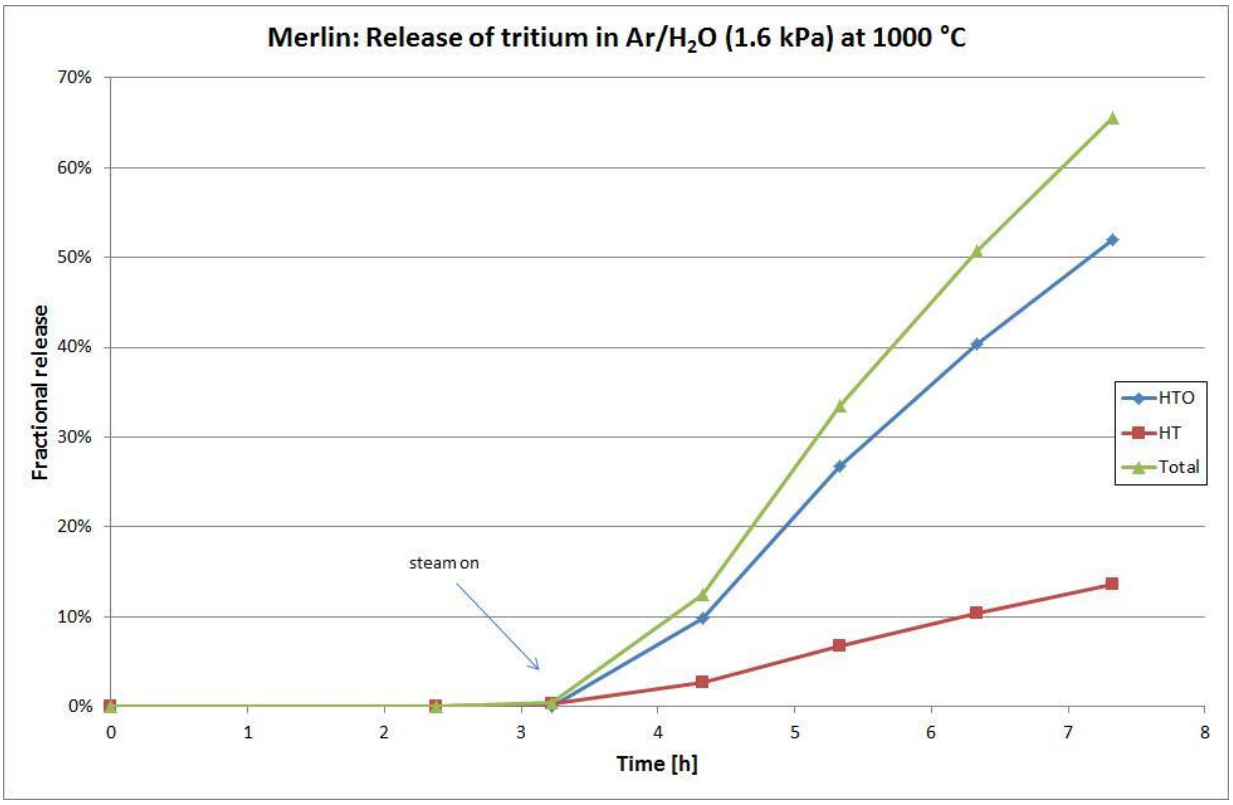


Figure 4.9: Estimated release of ^{3}H of Merlin-3 sample

There is no great difference in the release of ^{3}H, so it can be concluded that most of the release is based on the isotope-exchange and is transferred away as HTO and/or HT with the gas flow. Concerning Merlin-3 the lower release rate could be explained with missing absorbing HNO_3 in one of the bubblers.

Since there is high release rate of ^{3}H the released amount of ^{3}H in the second treatment is much lower - it is around 15 %.

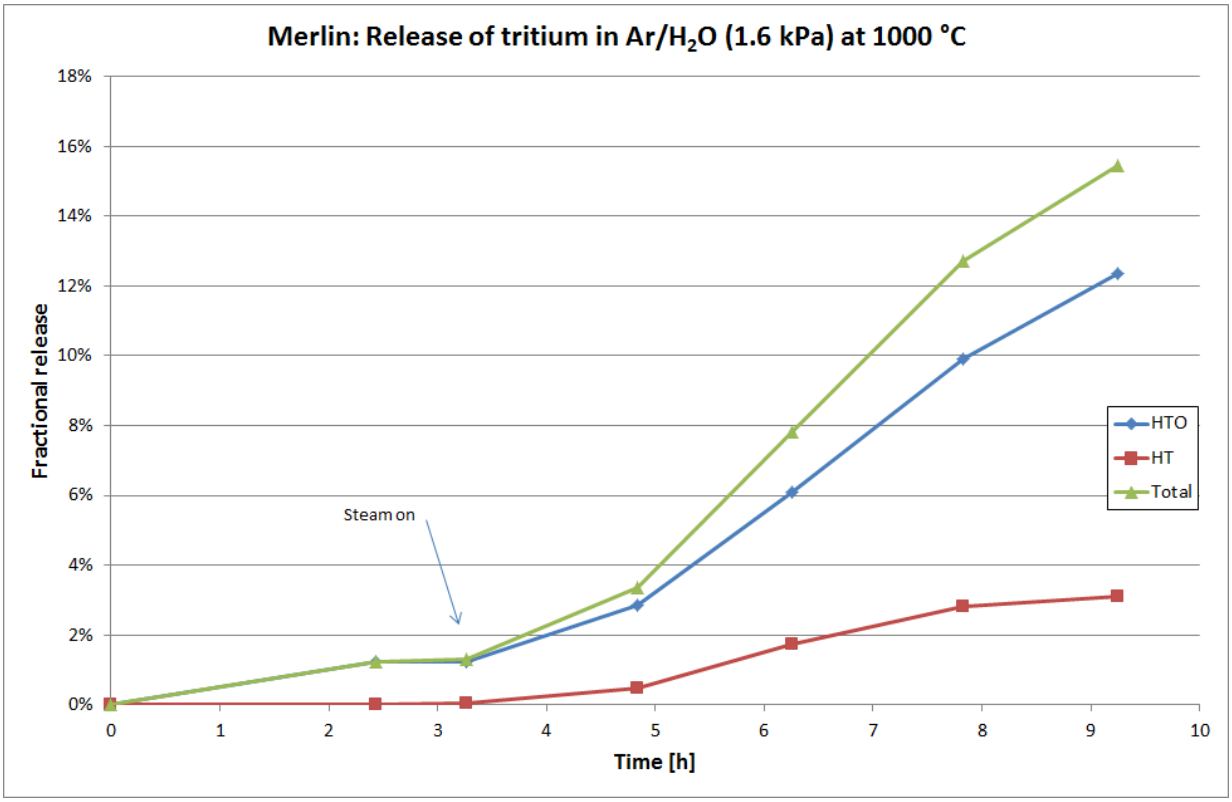


Figure 4.10: Release of ^{3}H of Merlin-2 in the second treatment

4.3.4 Mass spectrometer results

The mass spectrometer has shown that release of radionuclides is taking place even in the heating phase, but it is very low compared to the isothermal treatment phase with WetSys.
One can observe the huge amount of H_2O provided by WetSys within the isothermal phase. As a consequence of that the so called water-gas reaction with graphite is taking place.
Due to the instabilities of the flow the provided water is not stable during the experiment: it is raising. The gaseous emissions of CO and H_2 (see Chapter 2.3.2) are following this trend.
Moreover, an approximately constant emission of CO_2 can be observed, which could be caused by two origins:

- water gas shift reaction
- air ingress during the experiment, leading to the formation of CO_2

In addition one can see that the concentration of H_2 is higher than of CO and CO_2:

- CO_2 (brown line): 410 ± 20 ppm
- CO (red line): 760 ± 20 ppm
- H_2 (violet line): 1200 ± 20 ppm

This can be explained by the water gas shift reaction and the high amounts of water (blue line): a part of the H_2 can come from the water. It was not possible to separate these two effects completely. Therefore, it is likely that an overlapping of these effects was measured (see Figure 4.11).
Successive experiments with the Carbolite STF 15/-/180 (which are not part of this thesis) have revealed an air ingress of up to 15 ppm, but without using WetSys.

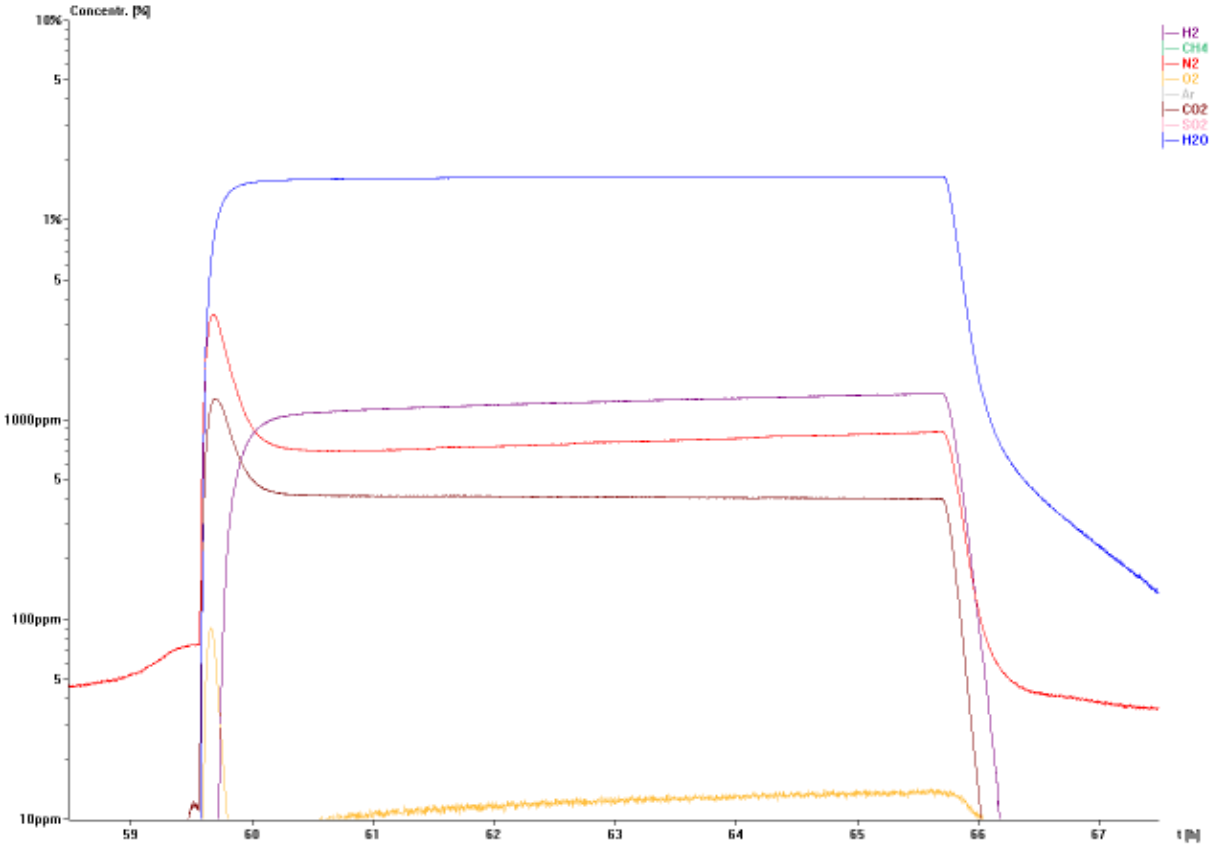


Figure 4.11: Concentration (semi logarithmic) of all gases of Merlin-3, second treatment

4.3.5 Determination of decontamination factors

The decontamination factor is a measure of the effectiveness of a decontamination process. It is the ratio of the original contamination to the remaining radiation after decontamination. A value of 1000 and above is excellent; 10 and below is poor [HUT].
The decontamination factors (DF) are determined with the following formula:

$$DF = \frac{A_{untreated}}{A_{treated}}$$

The activities $A_{untreated}$ and $A_{treated}$ are measured separately for ^{14}C and ^{3}H in Bq/g.

- $A_{treated}$ is the rest activity measured with LSC after combusting the treated sample in O_2
- $A_{untreated}$ is the sum of the rest activity and the activity released in the treatments

Subtracting the background is not necessary because this was already done in a previous calculation step.

Sample	Treatment gas	ϑ [°C]	Treatment time [h]	
			Heating	Isothermal
Merlin-1	Ar + H_2O (1.6 kPa)	1000	3:15	4
Merlin-2	Ar + H_2O (1.6 kPa)	1000	3:15	10
Merlin-3	Ar + H_2O (1.6 kPa)	1000	3:15	10

Table 4.1: Experimental conditions

Sample	Before treatment		After treatment	
	A(^{3}H) [Bq/g]	A(^{14}C) [Bq/g]	A(^{3}H) [Bq/g]	A(^{14}C) [Bq/g]
Merlin-1	1.73 E+03	3.55 E+02	4.70 E+02	2.88 E+02
Merlin-2	1.62 E+03	3.56 E+02	1.20 E+02	2.62 E+02
Merlin-3	≈ 1.67 E+03	≈ 3.55 E+02	7.49 E+01	1.61 E+02

Table 4.2: Activity before and after steam reforming

Sample	Mass loss [%]	Release [%]					
		HTO	HT	^{3}H total	$^{14}CO_2$	^{14}CO	^{14}C total
Merlin-1	1.58	58.0	15.4	73.4	12.1	8.0	20.1
Merlin-2	3.66	74.4	18.2	92.9	16.3	12.7	29.0
Merlin-3 (after 4h)	1.48	≈ 51.9	≈ 13.6	≈ 65.5	≈ 9.3	≈ 5.7	≈ 15.0

Table 4.3: Mass loss and release of ^{3}H and ^{14}C

Sample	Decontamination factor	
	^{3}H	^{14}C
Merlin-1	3.7	1.2
Merlin-2	13.4	1.4
Merlin-3	≈ 22.3	≈ 2.2

Table 4.4: Decontamination factors of ^{3}H and ^{14}C

4.4 Experiments with irradiated Saint Laurent graphite

The thermal treatment experiment with steam as oxidizing agent was done with Saint Laurent graphite samples. It was prepared and settings were arranged like described in the previous chapters, adjusted by a few exceptions for the mass spectrometer.

4.4.1 Performance of experiments

While the experiment was running, it was observed by a mass spectrometer. This was done to determine the compounds of the atmosphere inside the oven. To ensure that no water was condensate out in the oven or piping, the oven was heated up to 200 °C where the mass spectrometer was set a baseline.
While the oven was flushed by Argon gas the composition of gases inside the oven were constantly changing to a certain point at which no O_2 or N_2 was detectible. Assuming that those gases are the first detectable gases provided by leakages, the oven was considered leakage free. The gas flow was set higher than in the previous experiments because of the mass spectrometer that needs a gas flow of at least 60 mL/min for a correct measurement.

4.4.2 Release of carbon-14

The release of ^{14}C begins around 600 °C at low rates like the water gas reaction predict. From that point the oxidizing agent H_2O benefits the release of ^{14}C. The release of ^{14}C is nearly linear after the starting phase and differs after treatment between the probed samples a little: SLA2 R1 sample released an amount of 6.9% and the SLA2 R4 sample just released an amount of 8.2%.
After 12 hours and 40 minutes the oven is cooling down again. At this moment the linearity stops and the released amount of ^{14}C is decreasing.
Again it was not possible to determine an end of release of ^{14}C after 10 hours of treatment.

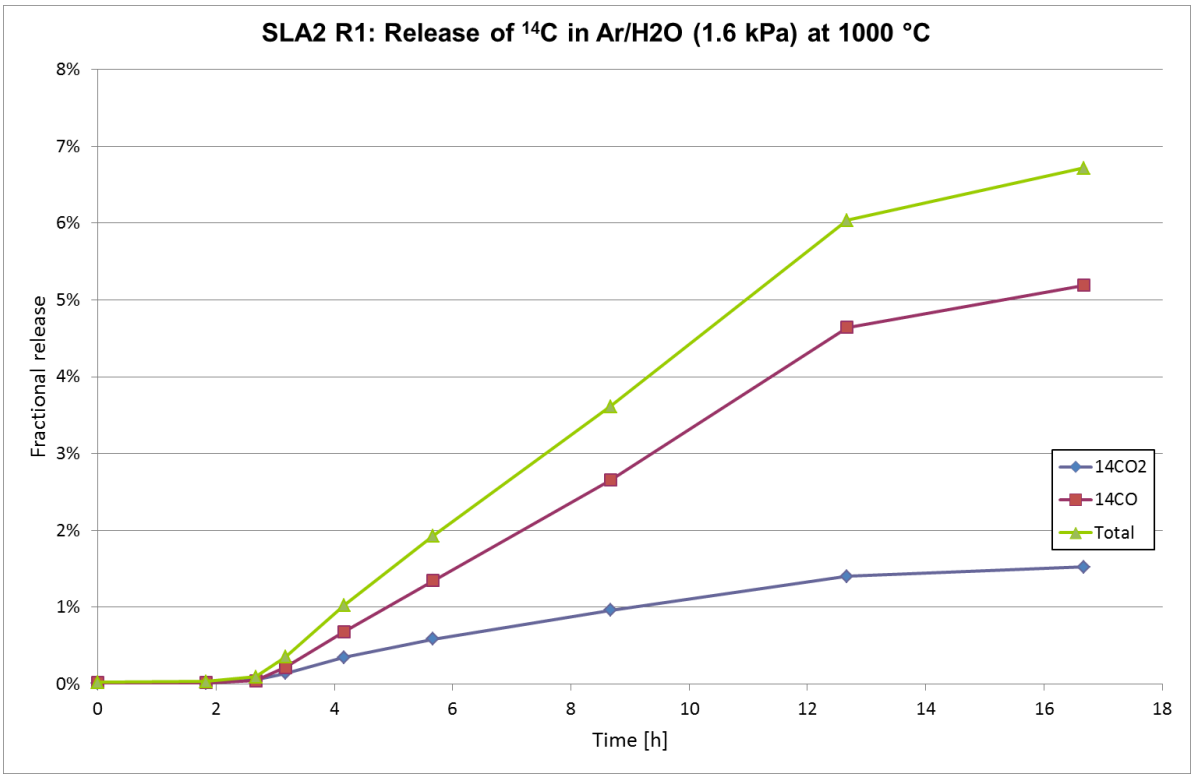


Figure 4.12: Release of ^{14}C of SLA2 R1 sample

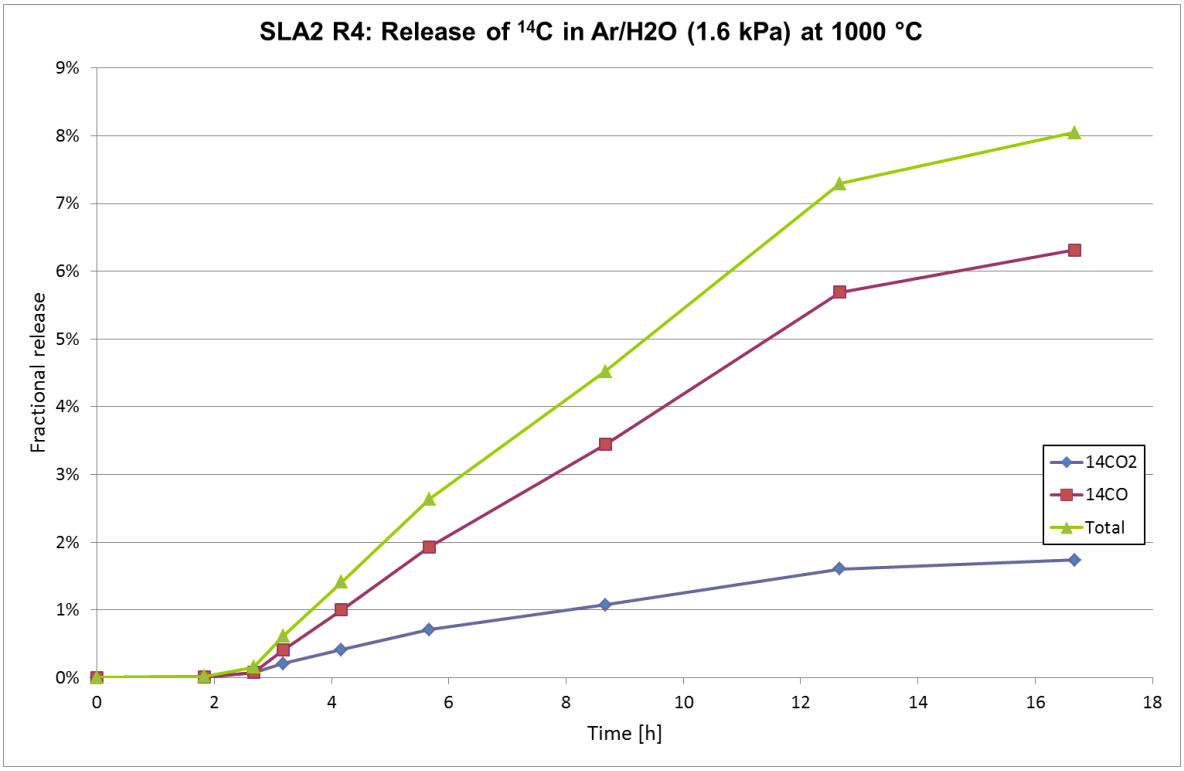


Figure 4.13: Release of ^{14}C of SLA2 R4 sample

4.4.3 Release of tritium

The release rates of tritium do differ around the same percentage amount as with ^{14}C. SLA2 R1 had a release of 39.7 % and SLA2 R4 had a release of 50.3 %. The release of tritium starts at the same time as ^{14}C is beginning to release. But in difference to ^{14}C it is not linear instead it raises high in the beginning and decreases over time.
After switching the heating of the oven off the tritium release is further decreasing. Nevertheless it was not possible to determine an end of release of tritium after 10 hours of treatment.

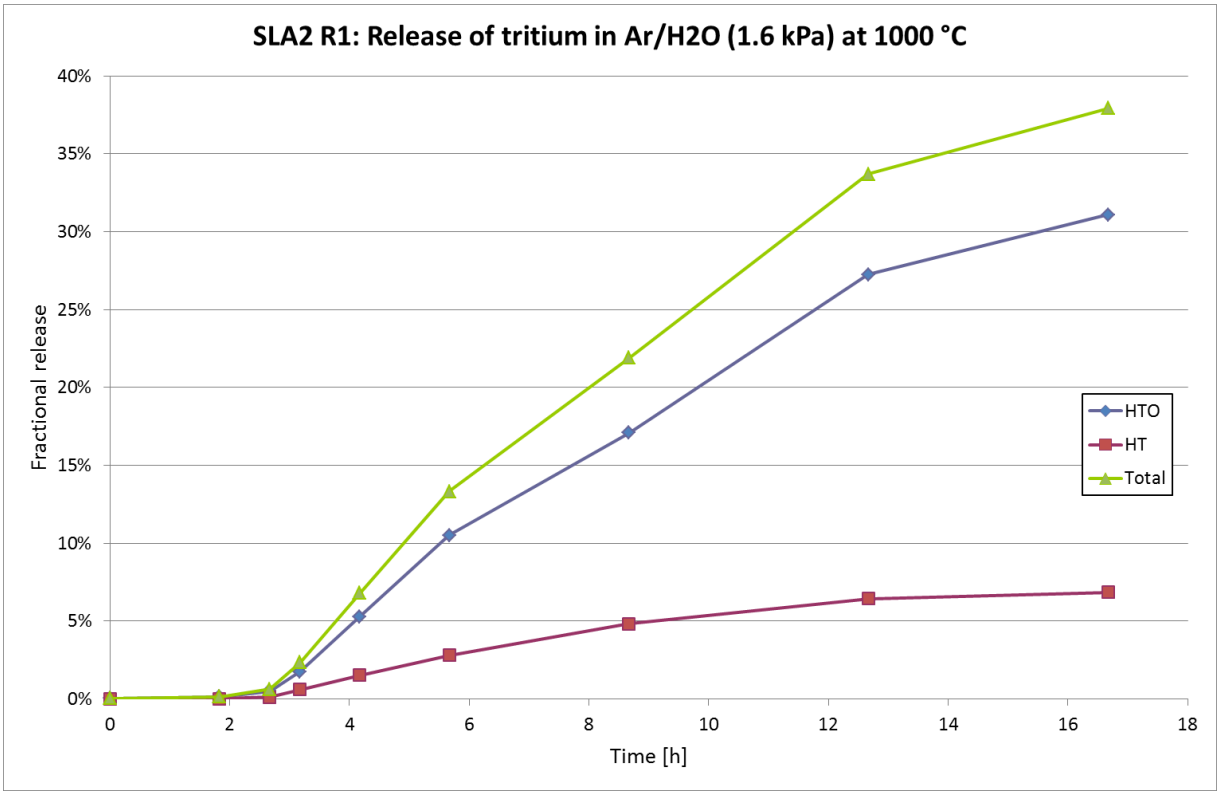


Figure 4.12: Release of tritium, SLA2 R1 sample

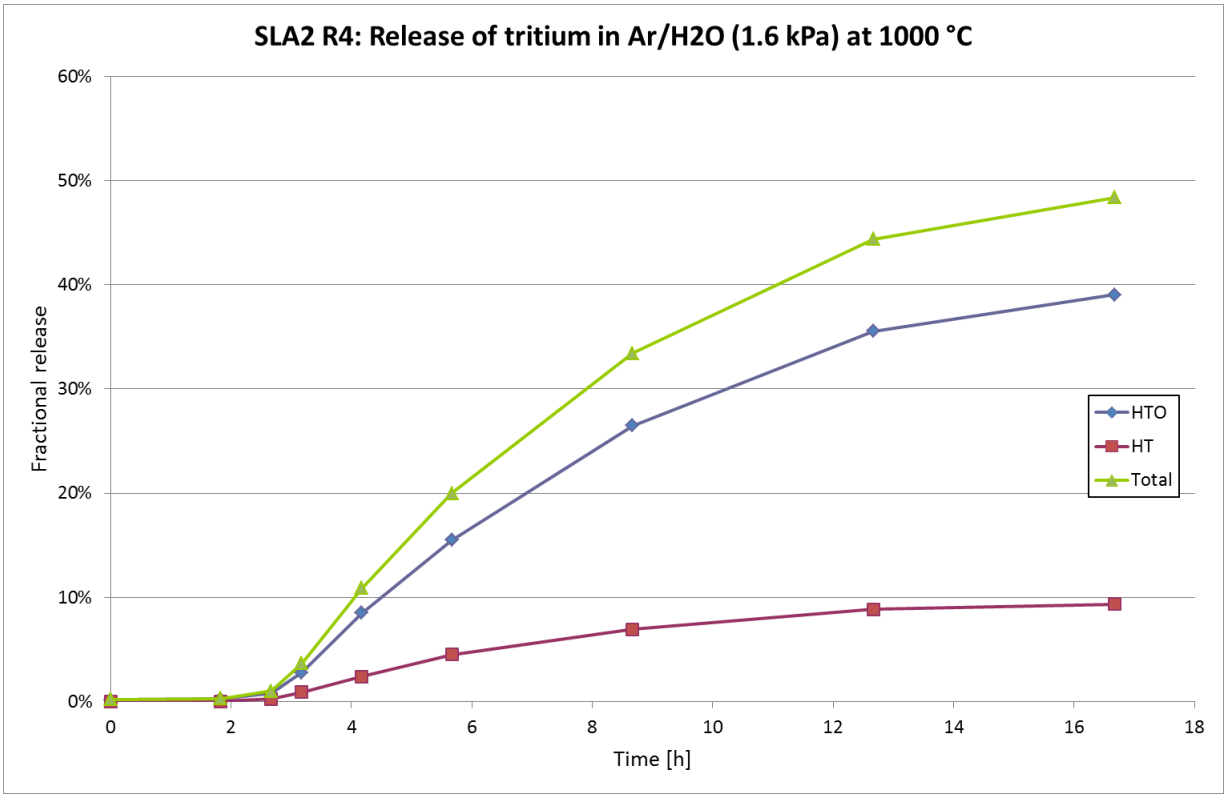


Figure 4.13: Release of tritium, SLA2 R4 sample

4.4.4 Determination of decontamination factors

The decontamination factor is a measure of the effectiveness of a decontamination process. It is the ratio of the original contamination to the remaining radiation after decontamination. A value of 1000 and above is excellent; 10 and below is poor [HUT].
The decontamination factors (DF) are determined with the following formula:

$$DF = \frac{A_{untreated}}{A_{treated}}$$

The activities $A_{untreated}$ and $A_{treated}$ are measured separately for ^{14}C and ^{3}H in Bq/g.

- $A_{treated}$ is the rest activity measured with LSC after combusting the treated sample in O_2
- $A_{untreated}$ is the sum of the rest activity and the activity released in the treatments

Subtracting the background is not necessary because this was already done in a previous calculation step.

Sample	Treatment gas	ϑ [°C]	Treatment time [h]	
			Heating	Isothermal
SLA2-R1	Ar + H_2O (1.6 kPa)	1000	2:40	10
SLA2-R4	Ar + H_2O (1.6 kPa)	1000	2:40	10

Table 4.5: Experimental conditions of SLA2

Sample	Before treatment		After treatment	
	A(^{3}H) [Bq/g]	A(^{14}C) [Bq/g]	A(^{3}H) [Bq/g]	A(^{14}C) [Bq/g]
SLA2-R1	9.64 E+04	5.19 E+04	5.94 E+04	4.04 E+04
SLA2-R4	1.40 E+05	6.82 E+04	7.10 E+04	4.93 E+04

Table 4.6: Activity before and after steam reforming of SLA2

Sample	Mass loss [%]	Release [%]					
		HTO	HT	^{3}H total	$^{14}CO_2$	^{14}CO	^{14}C total
SLA2-R1	2.16	32.6	7.1	39.7	1.6	5.3	6.9
SLA2-R4	2.20	40.7	9.7	50.3	1.8	6.4	8.2

Table 4.7: Mass loss and release of ^{3}H and ^{14}C of SLA2

Sample	Decontamination factor	
	^{3}H	^{14}C
SLA2-R1	1.62	1.05
SLA2-R4	1.97	1.06

Table 4.8: Decontamination factors of ^{3}H and ^{14}C of SLA2

5. Summary

The main goal of this deliverable was to establish decontamination factors of irradiated nuclear graphite's by steam reforming in order to set up an industrial prototype installation for graphite decontamination.

Before working with irradiated graphite, operation conditions were tested with virgin graphite samples. This step was necessary to see how the furnace would perform with graphite samples and if it could be used with the humidity generator WetSys. After finishing the experiments with non-irradiated graphite, the furnace outlet was connected to the bubblers in order to get to collect radionuclides, released.

The uncertainties of the measured data's were evaluated and are 3% for the tritium measurements and 10% for ^{14}C measurements. These uncertainties have to be taken into account by analyzing and interpreting the gathered data's.

After determining the experimental parameters for Merlin graphite:

- temperature of 1000 °C,
- absolute humidity of 10 g/kg
- 4 h (Merlin-1) respectively 10 h (Merlin-2, Merlin-3) of treatment and a
- gas flow of 25 mL/min,

the installation was ready to be loaded with irradiated graphite from the FRJ-1 Merlin reactor. Most of the experiments performed without any leakage or failure, leading to the following decontamination factors (DF) of the samples Merlin-1, Merlin-2 and estimated for Merlin-3:

Merlin-1

- $DF(^{3}H) = 3.7$
- $DF\ (^{14}C) = 1.2$

Merlin-2

- $DF\ (^{3}H) = 13.4$
- $DF\ (^{14}C) = 1.4$

Merlin-3

- $DF\ (^{3}H) \approx 22.3$
- $DF\ (^{14}C) \approx 2.2$

The decontamination factors are low, but are better than achieved with other methods (see A.2)! Nevertheless, there are still factors (temperature, humidity, treatment duration) which can be tuned to result in a better decontamination factor.

The second treatment of Merlin-3 sample with irradiated graphite failed. There was an uncontrolled gas leakage making it impossible to determine the amount of released radionuclides.

After determining the experimental parameters for Saint Laurent graphite:

- temperature of 1000 °C,
- absolute humidity of 10 g/kg
- 10 h (SLA2 R1, SLA2 R4) of treatment and a
- gas flow of 60 mL/min,

the installation was loaded with irradiated graphite from the Saint Laurent reactor.
The experiments were performed without any leakage or failure, leading to the following DF of the samples SLA2 R1 and SLA2 R4:

SLA2-R1

- DF(^{3}H) = 1.62
- DF (^{14}C) = 1.05

SLA2-R4

- DF (^{3}H) = 1.97
- DF (^{14}C) = 1.06

It is noticeable that a higher DF was achieved from the higher irradiated graphite. A temperature effect under irradiation could be a reason for this. But since SLA2 R1 was at 443°C and SLA2 R4 was at 391°C, no reactions are expected between CO_2 and graphite. Neutron radiation damage is expected, of course, higher for SLA2 R4 than SLA2 R1, since the R1 was in the middle of the core (h = 5120 mm) and the R4 was at the bottom (h = 1680 mm). In line of principle, a higher reactivity would be expected from the most irradiated sample due to the higher specific surface area caused by radiation damage.
It is very probable that the most significant influence on the reaction rates and removal behavior of ^{14}C and ^{3}H from SLA2 graphite is the radio lytic corrosion. This corrosion is higher in SLA2 R4 than in SLA2 R1 and correlates directly with the neutron fluence.
For what concerns ^{3}H, the DF for R1 is 1.62 against 1.97 for R4. Similarly, for ^{14}C, R1 showed a DF of 1.05 and R4 1.06. A higher decontamination could be correlated with higher neutron fluence.

However, it has to be underlined that the presented results are not significant from the statistic point of view and they cannot be considered as representative of the whole graphite in the same position in SLA reactor. Future investigations should focus on this topic in order to better characterize the graphite behavior in relation with its position in the reactor.

In conclusion, several conditions are heavily affecting the graphite behavior. Up to now, no literature reported a correlation among radio lytic corrosion and ^{3}H and ^{14}C removal. Further studies should focus on that way in order to better understand the removal mechanisms and radionuclide distribution inside the reactor in correlation with the history of the graphite. Another approach for the future would be to set a treatment time of more than 10 hours and focus the experiments to decontaminate the samples to a maximum amount in this given time of treatment, while using temperature and humidity levels as variables.

6. References

POD04 Graphite as radioactive waste: Corrosion behaviour under final repository conditions and thermal treatment
Jülich: Forschungszentrum (also dissertation RWTH Aachen) [Berichte des Forschungszentrums Jülich; 4166]
T. Podruzhina (2004)

DEL83 Graphitische Werkstoffe für den Einsatz in Kernreaktoren
Teil 2: Polykristalliner Graphit und Brennelementmatrix
München: Karl Thiemig AG
W. Delle, K. Koizlik, H. Nickel (1983)

FLO09 Dekontamination von Nukleargraphit durch thermische Behandlung
Dissertation RWTH Aachen
M.W. Florjan (2009)

WEI95 Identifikation von Beta-Nukliden und Analyse von Mehrfach-Beta-Spektren bei Messungen mit dem Flüssig-Szintillationsspektrometer (LSC)
Jülich: Forschungszentrum [Berichte des Forschungszentrums Jülich; 3066]
H.-J. Weise, P. Filss (1995)

KUG89 Hochtemperaturtechnik
Berlin u.a.: Springer
K. Kugeler, R. Schulten (1989)

FAC08 Decontamination of nuclear graphite
Nuclear Engineering and Design 238 (2008) 3086-3091
Elsevier B.V.
http://www.sciencedirect.com/science/article/pii/S0029549308001386
J. Fachinger, W. von Lensa, T. Podruzhina (2008)

EUR08 CARBOWASTE - Annex I ”Description of work”
EURATOM (2008)

FIS12 Gewichtsverlustbestimmung von nicht radioaktivem Graphit bei divergenter thermischer Behandlung, sowie Auslegung der TGA für die Messungen mit aktiviertem Graphit
Diplomarbeit FH Köln
C. Fischer (2012)

FZJ1 Forschungszentrum Jülich (Research Center Jülich) FRJ-1 Merlin
http://www.fz-juelich.de/gn/DE/Leistungen/NukleareProjekte/VorhabenProjekte/FRJ-1/Forschungsreaktor_MERLIN.html

FZJ2 Forschungszentrum Jülich (Research Center Jülich) FRJ-2 DIDO
http://www.fz-juelich.de/gn/DE/Leistungen/NukleareProjekte/VorhabenProjekte/FRJ-2/frj-2_node.html

FZJ3 Forschungszentrum Jülich (Research Center Jülich) FRJ-2 Dismantling
http://www.fz-juelich.de/portal/DE/UeberUns/Verantwortung/Aktuelles/doc/12-09-28dido-rueckbau.html

BfS Bundesamt für Strahlenschutz (Federal Office for Radiation Protection)
http://www.bfs.de/en/endlager/einfuehrung.html

HUT Hutchinson Encyclopaedia
http://www.talktalk.co.uk/reference/encyclopaedia/hutchinson/m0025923.html

A. Appendix

A.1 Activity inventories of other nuclear graphites

A.1.1 Irradiated DIDO graphite

Radionuclides	Activity [Bq/g]	Half-life [a]
^{3}H	2.4 E+06	12.32
^{14}C	9.8 E+04	5730
^{55}Fe	6.9 E+03	2.73
^{60}Co	7.4 E+03	5.27
^{90}Sr	0.0 E+00	28.5
^{134}Cs	2.7 E+02	2.1
^{137}Cs	7.5 E+01	30.2
^{133}Ba	1.8 E+02	10.54
^{152}Eu	0.0 E+00	13.3
^{154}Eu	2.3 E+03	8.8
^{155}Eu	1.3 E+03	4.8

Table A.1: Activity of DIDO graphite (Date: June 15, 2011)

A.1.2 Irradiated Merlin graphite

Radionuclides	Activity [Bq/g]	Half-life [a]
^{3}H	1.5 E+03	12.32
^{14}C	4.3 E+02	5730
^{55}Fe	3.3 E+01	2.73
^{60}Co	2.7 E+00	5.27
^{90}Sr	0.0 E+00	28.5
^{134}Cs	0.0 E+00	2.1
^{137}Cs	0.0 E+00	30.2
^{133}Ba	9.9 E+00	10.54
^{152}Eu	4.9 E+02	13.3
^{154}Eu	2.6 E+01	8.8
^{155}Eu	0.0 E+00	4.8

Table A.2: Activity of Merlin graphite (Date: June 15, 2011)

A.1.3 Irradiated Saint-Laurent A2 graphite

Radionuclides	Activity [Bq/g]	Half-life [a]
^{3}H	3.4 E+04	12.32
^{14}C	4.4 E+04	5730
^{55}Fe	0.0 E+00	2.73
^{60}Co	3.3 E+04	5.27
^{90}Sr	0.0 E+00	28.5
^{134}Cs	1.1 E+01	2.1
^{137}Cs	6.9 E+01	30.2
^{133}Ba	8.9 E+01	10.54
^{152}Eu	0.0 E+00	13.3
^{154}Eu	1.5 E+02	8.8
^{155}Eu	4.2 E+01	4.8

Table A.3: Activity of Saint-Laurent A2 graphite (Date: June 15, 2011)

A.1.4 Irradiated RBMK graphite

Radionuclides	Activity [Bq/g]	Half-life [a]
^{3}H	0.0 E+00	12.32
^{14}C	2.4 E+04	5730
^{54}Mn	2.1 E+00	0.86
^{55}Fe	0.0 E+00	2.73
^{60}Co	3.1 E+01	5.27
^{90}Sr	0.0 E+00	28.5
^{134}Cs	0.0 E+00	2.1
^{137}Cs	6.7 E-01	30.2
^{133}Ba	0.0 E+00	10.54
^{152}Eu	0.0 E+00	13.3
^{154}Eu	0.0 E+00	8.8
^{155}Eu	0.0 E+00	4.8

Table A.4: Activity of RBMK graphite (Date: June 15, 2011)

A.2 Summary of thermal treatment with decontamination factors

Exp. No.	Sample	Irradiation conditions		Experimental conditions			Mass loss [%]	Release [%]					Decontamination factor[4]	
		Cool. gas	T [°C]	Treat. gas	T [°C]	Treatment time [h] Heating	Treatment time [h] Isothermal		HTO	HT	^{3}H total	$^{14}CO_2$	^{14}CO	^{14}C total	^{3}H	^{14}C
V4	Merlin	Air	RT	N_2 + 0.14% O_2[1]	1300	0	10	0.89	85.9	7.7	93.6	3.4	2.5	5.9	15.4	1.05
V5	Merlin	Air	RT	N_2 + 1% O_2	900	3	2.5	6.64	10.1	0.2	10.3	8.6	3.3	11.9	1.04	1.06
V6	Merlin	Air	RT	N_2 + 1% O_2	700	2.5	7.75	7.22	26.5	0.2	26.7	14.5	7.3	21.8	1.26	1.19
V7	SLA2 9260	CO_2	258.5	N_2 + 0.14% O_2[1]	1300	0	10.5	0.91	65.0	0.2	65.2	1.4	0.6	2.0	2.85	1.01
V8	Merlin	Air	RT	N_2 + x% O_2[2]	1300	0	21	5.12	65.6	31.3	96.9	2.5	8.2	10.7	30.4	1.06
V9	Merlin	Air	RT	Pure N_2	1100	3.75	20	0.20	4.6	56.3	60.9	0.12	2.0	2.1	2.55	1.02
V10	Merlin	Air	RT	Pure N_2	1100	3.75	25.5	0.01	1.2	0.09	1.3	1.5	1.3	2.8	1.01	1.03
V11	Merlin	Air	RT	Pure N_2	1100	3.75	20.5	0.16	15.2	21.1	36.3	0.6	1.4	2.1	1.57	1.02
V12	SLA2 9260	CO_2	258.5	Pure N_2	1100	3.75	20.5	0.45	13.3	7.3	20.6	0.4	2.0	2.4	1.25	1.02
V13	Magnox	CO_2	270	Pure N_2	1100	3.75	11	0.14	1.8	0.8	2.6	0.5	1.9	2.4	1.02	1.02
V14	Merlin	Air	RT	N_2 + 0.1% O_2[3]	750	2.5	5	0.22	1.1	0.1	1.2	0.8	0.4	1.2	1.01	1.01
V15	Magnox	CO_2	270	N_2 + 0.1% O_2[3]	900	3	5	0.70	2.9	0.3	3.2	61.7	38.3	100,0		
V16	Magnox	CO_2	270	N_2 + 0.3% O_2[3]	900	3	5	3.90	4.8	0.05	4.9	3.1	1.5	4.6		
V17	Merlin	Air	RT	N_2 + 0.3% O_2[3]	900	3	5	1.62	30.0	0.07	30.1	9.9	4.1	14.0	1.41	1.14
V18	Merlin	Air	RT	N_2 + 0.3% O_2[3]	900	3	5	2.72	33.0	0.4	33.4	4.7	0.9	5.6	1.46	1.03
V19	SLA2 9260	CO_2	258.5	N_2 + 0.3% O_2[3]	900	3	5	2.43	2.8	0.02	2.8	2.1	0.5	2.6		
Merlin-1	Merlin	Air	RT	Ar + steam (1.6 kPa)	1000	3.25	4	1.58	58.0	15.4	73.4	12.1	8.0	20.1	3.69	1.23
Merlin-2	Merlin	Air	RT	Ar + steam (1.6 kPa)	1000	3.25	10	3.64	74.7	18.2	92.9	16.3	12.7	29.0	13.4	1.36
FH1	SLA2 5120	CO_2	391.5	Ar	1000		40	0.70			29.4			2.4		

RT = Room temperature
Red values: Determined by assuming an averaged initial radionuclide content

[1] Ceramic tube with measured ingress of O_2
[2] New ceramic tube, unknown ingress of O_2
[3] Quartz tube with defined amount of O_2 in the treatment gas
[4] The ratio of initial specific radioactivity to final specific radioactivity resulting from a separation process [McGraw-Hill: Dictionary of Scientific and Technical Terms]. 1000 and above is excellent; 10 and below is poor [Hutchinson encyclopaedia].

Date: December 17, 2012

A.3 List of figures

Figure 2.1	α-Graphite and β-graphite	7
Figure 2.2	Polycrystalline graphite mold	9
Figure 2.3	Scheme of FRJ-1 Merlin	10
Figure 2.4	Scheme of FRJ-2 DIDO	11
Figure 2.5	AVR graphite and carbon installations	12
Figure 2.6	Arrhenius diagram of corrosion ranges	19
Figure 2.7	Diagram of chemical reaction and concentration trend of reaction gas	20
Figure 2.8	Diagram of pore diffusion and concentration trend of reaction gas	20
Figure 2.9	Diagram of boundary layer diffusion and concentration trend of reaction gas	21
Figure 3.1	A double bubbler and a special designed sample holder made by ZAT	22
Figure 3.2	A sketch of the treatment installation	23
Figure 3.3	DIDO graphite sample	25
Figure 3.4	Merlin graphite sample	25
Figure 3.5	Packard Liquid Scintillation Analyzer Tri-Carb 2770 TR/SL	28
Figure 4.1	Mass loss over time	29
Figure 4.2	Mass loss at different temperatures	30
Figure 4.3	Release of ^{14}C of Merlin-1 sample	33
Figure 4.4	Release of ^{14}C of Merlin-2 sample	33

Figure 4.5 Estimated release of ^{14}C of Merlin-3 sample 34
Figure 4.6 Release of ^{14}C of Merlin-2 sample in the second treatment 35
Figure 4.7 Release of ^{3}H of Merlin-1 sample 36
Figure 4.8 Release of ^{3}H of Merlin-2 sample 36
Figure 4.9 Estimated release of ^{3}H of Merlin-3 sample 37
Figure 4.10 Release of ^{3}H of Merlin-2 in the second treatment 38
Figure 4.11 Concentration (semi logarithmic) of all gases of Merlin-3, second treatment 39
Figure 4.12 Release of ^{14}C of SLA2 R1 sample 48
Figure 4.13 Release of ^{14}C of SLA2 R4 sample 48
Figure 4.12 Release of tritium, SLA2 R1 sample 49
Figure 4.13 Release of tritium, SLA2 R4 sample 50

A.4 List of tables

Table 2.1 Impurities of AVR graphite 15
Table 2.2 Total activity of AVR graphite 16
Table 3.1 Merlin graphite samples 25
Table 3.2 WetSys parameters 26
Table 4.1 Experimental conditions 45
Table 4.2 Activity before and after treatment 45
Table 4.3 Mass loss and release of ^{3}H and ^{14}C 46
Table 4.4 Decontamination factors of ^{3}H and ^{14}C 46

Table 4.5 Experimental conditions SLA2 51

Table 4.6 Activity before and after steam reforming of SLA2 51

Table 4.7 Mass loss and release of ^{3}H and ^{14}C of SLA2 51

Table 4.8 Decontamination factors of ^{3}H and ^{14}C of SLA2 51

Table A.1 Activity of DIDO graphite 57

Table A.2 Activity of Merlin graphite 57

Table A.3 Activity of Saint-Laurent A2 sample 58

Table A.4 Activity of RBMK sample 58